SBS BASED SLOW-LIGHT GENERATION IN PHOTONIC CRYSTAL FIBER

A DISSERTION
SUBMITTED TOWARDS THE PARTIAL FULFILLMENT OF THE REQUIREMENTS FOR THE AWARD OF DEGREE OF MASTER OF TECHNOLOGY
IN
NANO SCIENCE AND TECHNOLOGY

SUBMITTED BY

SANDEEP YADAV
2K14/NST/22

UNDER THE SUPERVISION OF

Dr. AJEET KUMAR
ASSISTANT PROFESSOR

DEPARTMENT OF APPLIED PHYSICS
DELHI TECHNOLOGICAL UNIVERSITY
(FORMERLY DELHI COLLEGE OF ENGINEERING)
BAWANA ROAD DELHI 110042

JUNE 2016

SBS Based Slow-Light Generation in Photonic Crystal Fiber

A Dissertation submitted towards the partial fulfillment of
the requirement for the award of degree of

Master of Technology in
Nano Science and Technology

Submitted by
Sandeep Yadav
2K14/NST/22

Under the supervision of
Dr. Ajeet Kumar
Assistant Professor

Department of Applied Physics
Delhi Technological University
(Formerly Delhi College of Engineering)

JUNE 2015

DELHI TECHNOLOGICAL UNIVERSITY
Established by Govt. Of Delhi vide Act 6 of 2009
(Formerly Delhi College of Engineering)
SHAHBAD DAULATPUR, BAWANA ROAD,
DELHI-110042

CERTIFICATE

This is to certify that work which is being presented in the dissertation entitled

"SBS Based Slow-Light Generation in Photonic Crystal Fiber" is the authentic work of **Sandeep Yadav** under my guidance and supervision in the partial fulfillment of requirement towards the degree of **Master of Technology in Nano Science and Technology**, Department of Applied Physics in Delhi Technological University during the year 2014-2016.

As per the candidate declaration this work has not been submitted elsewhere for the award of any other degree.

Dr. Ajeet Kumar
Supervisor, Assistant Professor
Department of Applied Physics

Prof. S.C. Sharma
Professor
Head Department of Applied Physics
Delhi Technological University

DECLARATION

I hereby declare that all the information in this document has been obtained and presented in accordance with academic rules and ethical conduct. This report is my own, unaided work. I have fully cited and referenced all material and results that are not original to this work. It is being submitted for degree of Master of Technology in Nano Science and Technology at Delhi Technological University. It has not been submitted for any degree or examination in any other university.

Sandeep Yadav
M. Tech (NST)
2K14/NST/22

ABSTRACT

In today's world, the demand of ultra-fast information transfer with ultra-high bandwidths has reached to an extraordinary level. Hence, the transmission in the future internet-backbone will be constrained mostly in the network nodes. Also the power consumption of the network system will increase to indefensible levels. To overcome these constraints power-efficient photonic networks which can provide ultra-fast all-optical switching and routing are necessary. Optical buffering is required for such ultra-fast networks to avoid congestion.

Slow-light effect has been investigated as one of the solution of optical buffering. It means slowing down the group velocity of light pulses in a medium. To realize this, many different methods and materials have been developed but due to its significant advantages the nonlinear effect of stimulated Brillouin scattering (SBS) is particularly promising.

In this thesis, two different designs of photonic crystal fibers have been proposed for slow-light analysis. The first design is of rectangular core nature with inner air holes having more radius as compared to rest of the air holes. The material used for that design is Tellurite for 100 m long photonic crystal fiber. Another design has been designed with graded index feature *i.e.* the radius of the air holes keeps on increasing in a regular pattern. The analysis in this fiber has been done for 1 m long photonic crystal fiber with As_2Se_3 chalcogenide as material of the photonic crystal fiber.

Fundamental properties such as confinement loss and effective mode area for both the designs have been simulated. Using those parameters, a maximum time-delay of 154.3 ns has been reported for the first design having tellurite material. The power requirement found to be 26 mW to achieve such high time delay for the length of 100 m long photonic crystal fiber. A Brillouin Gain of 19.07 dB has been reported for that design. For the second design having chalcogenide material, maximum time-delay of 252.8 ns has been reported for 1 m long photonic crystal fiber for a small input pump power of 9.8 mW. The Brillouin Gain achieved for this design was also more as compared to the first design *i.e.* 99.78 dB. Both the designs were thus compared for slow-light using SBS effect.

Key words: Photonic crystal fiber, Confinement Loss, Effective Mode Area, Time-delay, Pump Power, Brillouin Gain

LIST OF RESEARCH PRESENTATION AND PUBLICATIONS

1. **Sandeep Yadav**, Than Singh Saini, Ajeet Kumar, " Slow Light Generation in Single-Mode Rectangular Core Photonic Crystal Fiber", *International Conference on Condensed Matter and Applied Physics (ICC 2015), AIP Conf. Proc.* 1728, 020389-1–020389-4; doi: 10.1063/1.4946440.

2. **Sandeep Yadav**, Than Singh Saini, Ajeet Kumar, "Stimulated Brillouin Scattering Based Slow Light Generation in Rectangular Core Photonic Crystal Fiber", Journal of Modern Optics (Communicated-January 2016).

3. **Sandeep Yadav**, Than Singh Saini, Ajeet Kumar, R. K. Sinha, "SBS Based Tunable Slow-Light in a Novel Graded-Index Photonic Crystal Fiber: design and analysis", Optik-International journal for Light and Electron Optics (Communicated-June 2016).

ACKNOWLEDGEMENT

I take this opportunity as a privilege to thank all individuals without whose support and guidance I could not have completed my project successfully in this stipulated period of time.

First and foremost I would like to express my deepest gratitude to my supervisor **Dr. Ajeet Kumar**, Asst. Professor, Department of Applied Physics, for his invaluable support, guidance, motivation and encouragement throughout the period this work was carried out. I would also like to thank **Than Singh Saini**, Research Scholar, for valuable time and interest in this project. I am grateful to both for closely monitoring my progress and providing me with timely and important advice, their valued suggestions and inputs during the course of the project work.

I am deeply grateful to **Prof. S. C. Sharma** for his support and encouragement in carrying out this project.

I also wish to express my heart full thanks to the classmates as well as staff at Department of Applied Physics of Delhi Technological University for their goodwill and support that helped me a lot in successful completion of this project.

Finally, I want to thank my parents, brother and friends for always believing in my abilities and for always showering their invaluable love and support.

Sandeep Yadav
M. Tech. NST
2K14/NST/22

CONTENTS

List of Tables

List of Figures

Chapter-1
Introduction

1.1 Thesis Approach

This thesis consists of design of two different core photonic crystal fibers. One of them is designed in square core with the inner diameter of the air holes is more than the rest of the air holes of other layers. The other design is of graded nature in which the radius of the air holes is increasing continuously in a regular pattern. 'Comsol-Multiphysics' software which uses Finite–Element method to solve complex electromagnetic fields is used to design and to calculate the effective mode area and confinement loss of the fundamental mode of the photonic crystal fiber. Both the designed photonic crystal fibers are then analyzed for stimulated Brillouin scattering based slow-light. MATLAB software is used to calculate and plot the rest of the parameter like threshold power, the maximum time delay achieved, Brillouin Gain and figure of merit.

1.2 Thesis Objective

The main objectives of the thesis are mentioned below:

1. To study the classification, basic properties of photonic crystal fiber such as single mode operation, dispersion, large mode area and birefringence.
2. To study various method used for achieving slow-light in any fiber such as waveguide-loop method, electromagnetically induced transparency (EIT) method, coherent population oscillation (CPO) method, Quasi-light storage (QLS) method and stimulated Brillouin scattering (SBS) method.
3. Design and analysis of Stimulated Brillouin Scattering Based Slow Light Generation in Rectangular Core Photonic Crystal Fiber.
4. Design and analysis of SBS Based tunable slow-light in a novel graded-Index photonic crystal fiber.

1.3 Thesis Organization

This thesis has been organized into 6 chapters. Chapter 1 deals with the introduction and objective of the thesis. The literature review, historical developments properties of photonic crystal fiber and their applications are well described in chapter 2. Chapter 3 is regarding various methods to achieve slow light such as EIT, CPO, QLS and SBS are explained with their advantages and its applications. In chapter 4, we have presented our designed model of the photonic crystal fiber with tellurite as material and calculated various parameters required examining the time delay introduced by the designed photonic crystal fiber. Another model designed by us was a graded index photonic crystal fiber with chalcogenide material has been explained in chapter 5 with all the parameters required to examine the slow-light. In chapter 6 the work carried out has been concluded and future scope regarding this field is mentioned.

Chapter-2
Photonic Crystal Fibers

2.1. Introduction

The optical fibers have revolutionized the field of telecommunications in past few decades [1]. In spite of their excellent performance in transmission of optical signals, the advancement in optical technology have reached to its ultimate limit as the intrinsic properties of silica have forced fundamental restriction on the performance of conventional optical fibers. As they have strict design rules to accomplish like limited core diameter for single mode operation, cut-off wavelength, and restriction in material selection as the core and cladding must have matching thermal properties. Also the restriction on geometry and refractive index profile of the conventional fiber obstruct the flexibility in engineering fiber properties such as dispersion, nonlinearity and birefringence for better performance and good application. Another drawback of the optical fiber was that when the light travels through it, it suffers losses & attenuation due to material absorption and Rayleigh scattering.

These limitations of conventional optical fibers led to the development of new class of optical waveguides known as the Photonic Crystal Fibers (PCFs). Photonic Crystal Fibers (PCFs) are fibers with an internal periodic structure made of capillaries running parallel to the fiber axis along the entire length of the PCF, filled with air, laid to form a (hexagonal, triangular, rectangular etc.) lattice. There were several advantages of designing PCF such as

- PCFs are made of single material reducing the need of two thermally, optically & chemically compatible glass to form core and cladding in conventional fibers.
- Great design flexibility
- Highly-engineerable refractive index profile lead to desirable birefringence, nonlinearity and chromatic dispersion.
- Lower losses

In this chapter we will have a brief historical overview of development of PCF in section 2.2, followed by classification and guidance mechanism of various classes of PCF in section 2.3. We will have an overview of the novel properties of the PCF in section 2.4 and applications of PCFs in section 2.5.

2.2. Historical overview

As many scientific inventions are inspired by living beings in nature, the photonic crystals of the PCFs have the similarities in the photonic stop-band based nanostructure in the wings of the butterflies (Fig. 1.1(a)) and the iridescent setae from polychaete worms (Fig. 1.1(b)) [2]. The periodic variation in PCF is same as the band structure of the semiconductors in which electrons interact with the periodic variation in the potential that is created by the atomic

crystal lattice. Melekhin and Manenkov in 1968 [3] and Yeh *et al*. in 1978 [4] were the first to use the idea of periodic one-dimensional variation in the dielectric to trap light. They proposed to clad a fiber core with a multilayer coating similar to that in planar Bragg stacks which results in light guidance in Bragg fiber. Yablonovitch [4, 5] from his studies predicted that certain dielectric structures can have a frequency band in which all the propagation modes are forbidden and termed those structures as photonic bandgap (PGB). Thus the light exists in forbidden bandgaps and propagates through the defects [6]. This mechanism leads immediate emission on photonic states in the lattice by having a three dimensional photonic crystal.

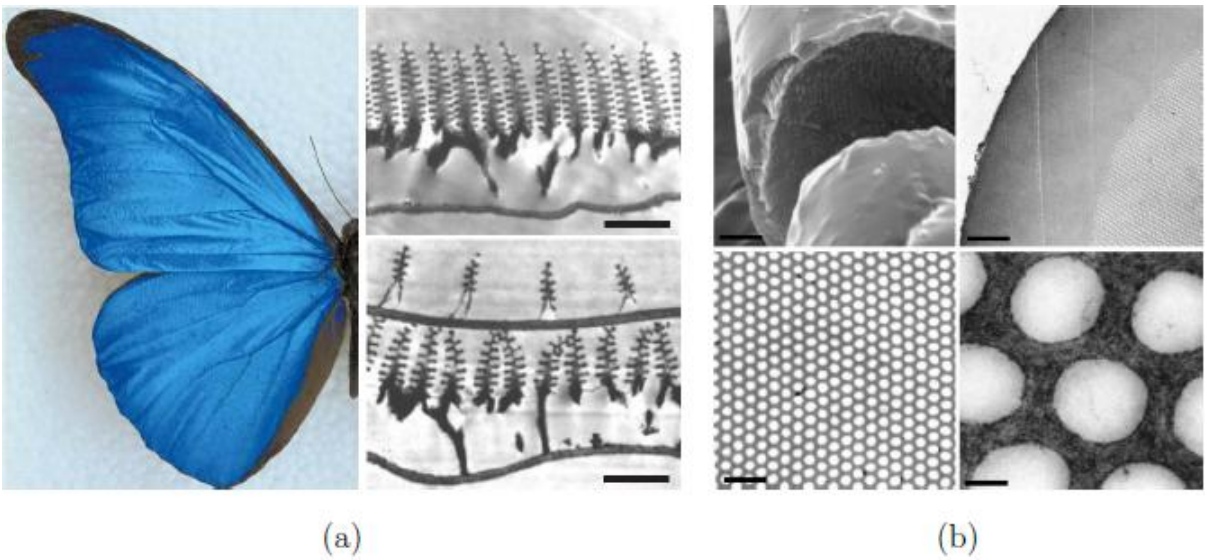

Fig.2.1: (a) Iridescence in the buttery *Morpho rhetenor* and transmission electron micrograph (TEM) images showing wing-scale cross-sections. Scale bars: 1.8 μm, 1.3 μm. (b) Iridescent setae from polychaete worms: scanning electron micrograph (SEM) and TEM images of transverse sections through a single iridescent seta. Scale bars: 2 μm, 5 μm, 1 μm, 120 nm (Source [2]).

The remarkable advancement of PCFs took place only in past few decades when the manufacturing technology become so advanced to fabricate a precise complex silica-air structures [7, 8]. *Birks et al.* in year 1995 proposed an optical fiber that can guide light in a hollow core by using photonic bandgap phenomenon [9]. The first index guiding PCF with periodic air silica cladding was proposed by *Knight et al*. in year 1996 [7, 8]. First experimental demonstration of photonic bandgap fiber with honeycomb structure took place in the year 1998 by *Knights et al*. [10]. In year 1999, *Kregan et al*. proposed a triangular cladding structure photonic bandgap fiber which can guide 98% of the power in the air-regions of the fiber [11].

Defects can also be introduced in two-dimensional photonic crystal slabs to form waveguides in same way as for three-dimensional photonic crystal. The guidance mechanism in two-dimensional photonic crystal is based on the photonic bandgap effect in the plane of periodicity and the light is confined perpendicular to this plane by index guidance mechanism. In case of PCFs, the light enters normal to the plane of the periodicity.

Some important developments in PCF have been enumerated in Table 1.1.

Year	PCF Development
1995	Hollow core fiber with photonic bandgap cladding [9]
1996	Demonstration of microstructured fiber with periodic air-silica cladding[7, 8]
1998	First demonstration of photonic bandgap fiber [10]
1998	Large Mode Area in photonic crystal fiber [12]
1999	Guidance of light in air in photonic bandgap fiber [11]
1999	Supercontinuum generation in microstructured fiber [13]
2000	Highly birefringent photonic crystal fibers [14]
2001	Four-wave mixing in microstructured fiber [15]
2002	Particle levitation and guidance in hollow-core photonic crystal fiber [16]
2003	Tellurite photonic crystal fiber [17]
2005	All-solid photonic bandgap fiber at 1% index contrast [18]

PCFs are different from photonic crystal waveguides which can be explained using the Bragg's law for constructive interference:

$$m\lambda = 2\Lambda cos\theta \qquad (2.1)$$

where m is an integer, λ is the wavelength of the incoming light, Λ is the pitch of the periodicity and θ is the incident angle of the incoming wave. In case of waveguides, $\theta = 0$ and Λ is of the order of λ of the incident light, whereas in case of PCFs, there is grazing incidence of the light and Λ is much larger than the wavelength of the incoming wave. Due to having smaller pitch, the waveguides have relatively higher losses as compared to PCFs; this makes the PCFs superior to the photonic crystal waveguides.

2.3. Classification and guidance mechanisms in PCFs

In a conventional fiber, light guidance is basically dependent on the difference in the refractive index of core and cladding having different doping levels. Whereas in PCFs the guidance of light is dependent on the optical confinement and it can be categorised into two classes as index-guiding fibers [7, 8, and 19] and bandgap-guiding fibers [10, 11, and 19]. Figure 2.2 shows the classification of the PCFs depending upon the guidance mechanisms.

2.3.1. Index-Guiding PCFs

Index-guiding PCFs are same as the conventional fibers and work on same total internal reflection phenomenon. These are the simplest kind of PCFs having a solid core made up of a highly refractive material such as silica, tellurite or chalcogenide. The air holes are present in a periodic arrangement [7, 8] or in a random arrangement in the fiber cladding [21]. Due to the presence of air holes in the cladding, the refractive index of the cladding get reduced which allows the guidance of light by total internal reflection as explained in fig.2.3. The index-guiding PCFs are also termed as Microstructured Fiber (MF) or Holey Fiber (HF). It can be further categorised depending upon its properties and use as shown in fig.2.2. Index fibers cannot be designed with a hollow core as it is mandatory for total internal reflection that the refractive index of the cladding material must be lower than the refractive index of the core material. These fibers have better performance and good properties as compared to that of the conventional fibers because these fibers has better properties such as it behaves as endlessly single mode fiber provided the air filling fraction (*i.e. d/Λ*) is very small.

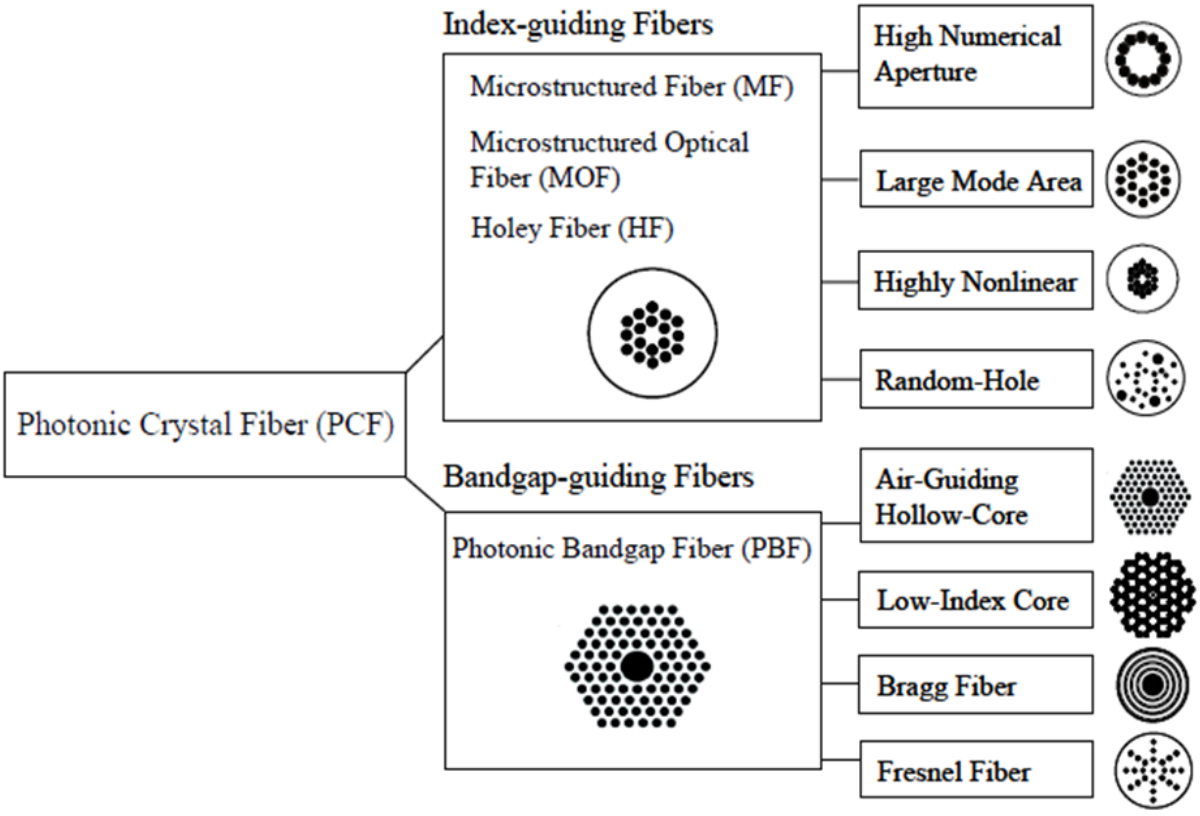

Fig.2.2: Classification of photonic crystal fibers (Source [20])

These PCFs has lesser optical losses, they can be fabricated to support large mode area which makes the suitable for development of fiber lasers and amplifiers.

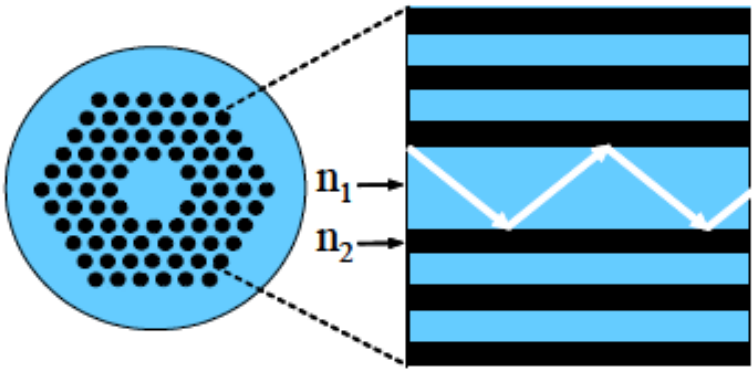

Fig.2.3: Total internal reflection phenomenon in an index-guiding PCF (Source: Ph.D. thesis: Tuomo Ritari, "Novel Sensor and Telecommunication Applications of Photonic Crystal fibers".)

2.3.2. Hollow-Core PCFs

The confinement of light in hollow-core PCFs or waveguides are either by total internal reflection [22, 23] or by reflection off a metallic surface [24]. They offer quasi-single-mode operation by guiding the light through the hollow-core made by the air, surrounded by the cladding which is formed by air and holes in silica material. Hollow-core PCFs supports multiple modes at any stated wavelength within the bandgap such as guided mode and surface mode. They can operate at higher-order modes but the problem is that they have much higher scattering and confinement losses as compared to the fundamental mode [25].

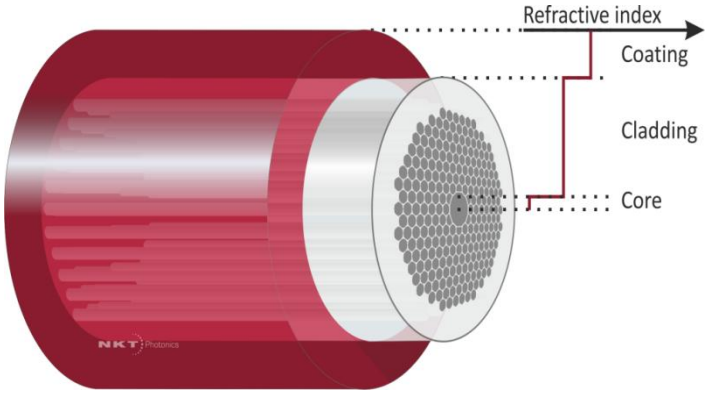

Fig.2.4: Hollow-core PCF (Source: NKT Photonics Website)

2.3.3. Photonic Bandgap PCFs

The another class of PCFs is Photonic bandgap fibers in which the periodic cladding microstructure results in a bandgap that can confine light inside the hollow core or in a core made up of the material having lower refractive index than that of the effective index of the cladding. Thus light can be guided in gas filled core [11, 26] or even in a solid core [27]. This phenomenon of guiding a light of finite frequency regions and not allowing to propagate

through the photonic crystal cladding is termed coherent Bragg scattering as shown in fig.2.4. Such fibers are known as photonic bandgap PCFs.

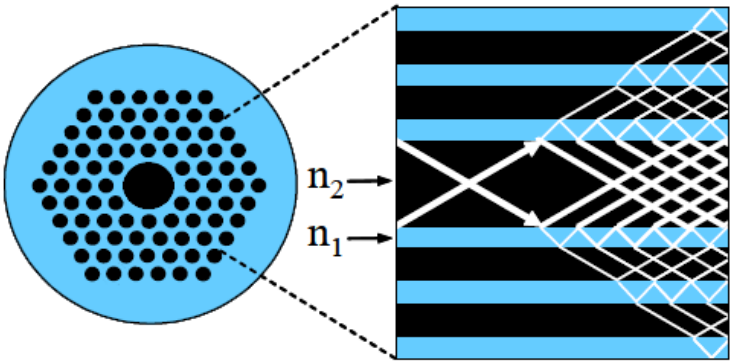

Fig.2.5: Coherent Bragg scattering phenomenon explaining the propagation of light in photonic bandgap PCFs (Source: Ph.D. thesis: Tuomo Ritari, "Novel Sensor and Telecommunication Applications of Photonic Crystal fibers".

2.3.4. Hybrid PCFs

Hybrid PCFs are special category of PCFs in which a single row of the air-holes are replaced by some other material such as germanium, tellurite or chalcogenide. Figure 2.6, shows the diagram of a germanium-doped silica and air holes around pure silica. Due to the replacement of the single row of air holes with germanium doped along one of the axes, makes the PCF a one dimensional photonic bandgap in that direction. If it is assumed the there is a hybrid PCF with a single row of germanium doped in x-direction, then the x-direction of the PCF core will have lower refractive index as compared to the cladding of the PCF, but along y-direction the effective refractive index of the core will remain higher than cladding. Thus it can be easily concluded that total internal reflection along x-direction is not possible whereas along the y-direction the PCF will show total internal reflection [28].

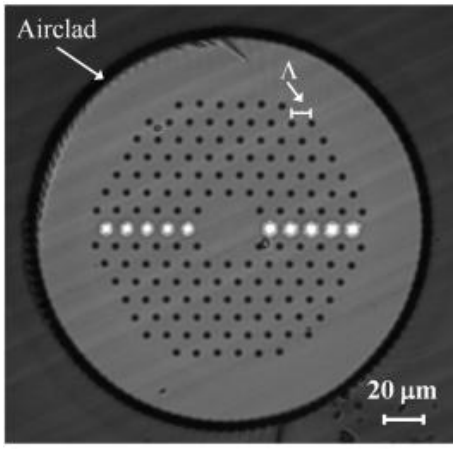

Fig.2.6: Microscope image of a silica double-clad large mode area hybrid PCF. The air-holes are placed in a hexagonal lattice and one of the air hole replaced by Germanium-doped silica rods. (Source: [29])

2.4. Properties of PCFs

2.4.1. Dispersion Properties

There are basically two types of dispersion, one is known as material dispersion and the other is waveguide dispersion. Material dispersion is dependent on the wavelength of the interacting light and the refractive index of the material of the core and the cladding [30-32] whereas the waveguide dispersion depends on the core diameter and the refractive index contrast between the core and cladding. In case of conventional optical fiber, the waveguide dispersion is of the order of material dispersion due to low index contrast between the core and the cladding.

The development of PCFs has made the new possibilities of controlling the dispersion of the PCFs. The dispersion of any PCF can be controlled by changing the pitch (Λ) and the air-hole size (d). High air-filling fraction (d/Λ) leads to strong waveguide dispersion, thus be properly choosing the structural parameters properly we can shift the zero-dispersion wavelength (λ_{ZD}) from near infrared to visible region [33].

2.4.2. Single-Mode Fiber

The PCFs were designed to operate in single mode over a large range of visible and near infrared spectrum. In case of normal step index fibers there is a cutoff frequency above which the fiber starts to operate in multimode. To find out the numbers of modes of any step index fiber, we use normalized frequency represented by V and is related to the refractive indices of the core and cladding as given by equation 2.2.

$$V = \frac{2\pi r}{\lambda}\sqrt{n_{core}^2 - n_{cladding}^2} \qquad (2.2)$$

where, r is the core radius, n_{core} and $n_{cladding}$ are the refractive indices of the core and cladding respectively. In case of conventional fibers, the refractive index of the cladding is wavelength and thus the value of V increases as the wavelength decreases which results to multimode operation of the fiber. The defined normalized cutoff frequency for multimode operation is found to be 2.405.

While in case of PCFs, the refractive index of the cladding is strongly reliant on the wavelength of the input light. Due to this dependence, the normalized frequency depends on the air filling fraction of the designed PCF. Air filling fraction of the PCF is the ratio of the diameter (d) of the air holes to the distance (pitch) between the centers of the air holes (Λ). If a PCF is designed appropriately, the value of V can be kept below the cutoff normalized frequency for any wavelength range. Hence they satisfy the condition of single mode. The cutoff normalized frequency for PCF has been estimated to be 2.5 [34, 35].

2.4.3. Large-Mode Area

Another drawback of conventional fibers is the limit of maximum core size and numerical aperture (NA) for working in single mode. There is always a maximum NA for any wavelength and core diameter for single mode operation and this NA is dependent on the difference in the refractive indices of the core and the cladding. To fabricate a large mode area single index fiber, it is required to control the refractive index in chemical vapor deposition with extremely high accuracy of 10^{-6} or more. Due to this, the mode field diameter (MFD) of the fiber gets limited in practice. MFD of the fiber can be defined as $1/e$ of width in intensity.

While in case of PCFs, MFD can be varied in a single mode regime as per the requirements. There are various methods to design a large mode area PCFs, some of them are as follows:

- Increasing the pitch of the air-holes in the cladding of the PCF.
- Decreasing the diameters of the air-holes in the cladding of the PCF.
- Increasing the size of the defect in the photonic cladding *i.e.* removing one more layer of the central air holes.

Bagget *et al*. [36] had shown that a large mode area single index fiber [SIF] and PCF can have similar MFD at any particular wavelength, provided the PCF has single capillary defect. It was analyzed that at higher range of frequencies, the PCFs remain in single mode whereas SIF starts to operate in multimode closer to designed wavelength. PCFs with larger MFD can be fabricated by replacing the air-holes with several rods. Bagget *et al*. [36] also band losses limits the performances of SIFs whereas it has no effect on PCFs.

2.4.4. Birefringence

Birefringence is the phenomenon of splitting of light into two inequitably reflected and transmitted waves by an anisotropic medium such as calcite or quartz. This phenomenon of splitting of light is also termed as double refraction. It basically results due to the small variation in the symmetry of the fiber or due to asymmetrical stress distribution. In a conventional fiber, Birefringence changes arbitrarily due to local fluctuation in core shape and stress distribution [31, 32]. The unique manufacturing process of the PCFs gives a good control over the cross-sectional index profile of the PCF, due to which birefringence in case of PCF remains constant all over the PCF. It is basically dependent on the asymmetrical core of the core or the cladding microstructure [14, 37] and found to be higher than the conventional fibers due to high contrast in PCF core and cladding refractive indices [38]. Due to the use of single fabrication material, the birefringence of the PCFs remains constant against the temperature variations. Also it is possible to induce stress birefringence in PCFs, which is quite helpful in realization of polarization-maintaining single-mode large-mode area fibers.

2.4.5. Nonlinearity

Due to developed manufacturing and fabrication techniques, it is possible to fabricate a PCF of very small core diameter and high air filling fraction. Due to which the effective mode area of the designed PCFs can be less as compared to the conventional fibers. From the equation given below, it can be concluded that the nonlinearity (γ) is inversely proportional to the effective node area of the PCF [30].

$$\gamma = \frac{2\pi n_2}{\lambda A_{eff}} \qquad (2.3)$$

where, n_2 is the nonlinear refractive index of the PCF, λ is the wavelength of the input wave and A_{eff} is the effective mode area of the PCF. Thus lower is the value of A_{eff}, higher will be the nonlinearity. Hence this nonlinearity can be combined with other dispersion properties of PCFs provides new possibilities in nonlinear optics. Also Aeff is dependent on the wavelength which can help in realization of wavelength dependent nonlinear effects [39].

2.4.6. Transmission loss

Fiber loss in any conventional fiber or photonic crystal fiber can be reduced by augmenting the structural uniformity as well as reducing material contamination and the surface roughness of the holes. In case of index-guiding PCFs the loss is comparable to the single mode conventional fibers, but in case of photonic bandgap PCFs the losses are less than conventional fibers because most of the light is guided in an air-core and hence losses are not limited by Rayleigh scattering and silica absorption in the same way as the conventional fibers [31, 40].

2.5. Applications of PCFs

The above mentioned novel properties of PCFs make them superior to the conventional fiber. Hence they are preferred more in many applications over these conventional optical fibers. Some of them as mentioned as follows:

2.5.1. Endlessly Single-Mode PCFs

As we all know that only a few geometries of PCFs support single-mode operation and also that its single-mode operation in such geometries is independent of the core size of the PCF and the wavelength of the propagating pulse. Hence they are termed as endlessly single-mode PCFs. This property of the PCF makes it suitable for various applications in single mode fiber lasers of low power and amplifier in optical fiber communications.

2.5.2. Large-Mode-Area PCFs

The power transmitting through the PCF is proportional to the mode area of the PCF. Higher is the mode area, higher is the power carrying capacity. This meant that large-mode-area property of the PCFs makes them suitable for high power use without any material damage

and nonlinear effects. This property of the PCF is quite useful in high power single mode fiber lasers and amplifiers.

2.5.3. Dispersion Compensating PCFs

Another major application of PCF is found in compensating the dispersion of the fibers means it can be used in dispersion tailoring devices. Initially fibers were designed to operate at 1.33 μm but now a day they are designed to operate at 1.55 μm due to which fibers have higher dispersion. Hence the PCFs are quite helpful in compensating the high order dispersion of the fibers. This property of the PCF makes it suitable for wavelength division multiplexing where compensation is required over a wide range.

2.5.4. Polarization Maintaining PCF

Birefringence in a PCF is due to the stress generated in PCF during the fabrication process. This property of PCF has an important effect in the transmission characteristics of the PCF. Another method of inducing Birefringence is bending and thermal effect and due to these effects, different optical axes are generated. When a plane polarized wave propagates along the PCF, get resolved into components along theses axes and propagates at different speeds. Due to difference in the phase, elliptically polarized light is generated and hence due to these phase mechanism, there is a delay in optical signals which is known as polarization mode dispersion (PMD). This PMD method is quite helpful for high transmission rates. Polarization maintaining PCFs are emerging as a new competitor for conventional polarization maintaining fibers. The advantage of PCFs over conventional fiber is that they remain in single-mode and hence they can transmit polarized light in a broad range of frequencies. Another advantage of using PCF over fiber is that it reduces bend induced coupling between the polarization states and improved excitation rate, it is basically due to smaller beat length of the PCFs as compared to conventional fibers. PCFs also have higher temperature coefficient of birefringence. Such properties of PCFs find applications in sensors gyroscopes and interferometers.

Chapter-3
Theory of Slow-light

3.1. Introduction

The velocity of light in vacuum is given by 'c' which is approximately 3×10^8 m/sec. The advantage of this ultrahigh speed of light is that the data transmission between two points whether they are separated on global scale or on a single chip, becomes efficient. While these lights are efficient but there is a problem in controlling these lights in time domain. Hence there is a need of 'slow light' to overcome this problem [41].

Slow-light is a key method for the potential alternates of electronic delay lines in telecommunications because such tunable delays helps in various digital signals processing functions that are very useful in communications systems. This method is quite helpful in accurate and fine control of an optical delay in high bit-rate systems such as time-divison-multiplexers, data equalization using tapped-delay-lines, and optical correlation where the control of light within fraction of time is very tough [42, 43]. There are many other applications of slow-light such as optical buffering, microwave photonics, optical memories, optical signal processing and precise interferometric instruments [44-46]. This technique also provides anticipative solution of broadband and tunable time-delay for microwave and milli-meter wave systems [47-48].

Slow light is basically defined as the light wave having very low group velocity. It is ultimately a technique that alters the propagation of pulses through any medium to generate unusual effects including time delay that refers to slow propagation velocities. As we all know that a monochromatic light travels at the phase velocity given by V_p

$$V_p = \frac{\omega}{k} = \frac{c}{n} \qquad (3.1)$$

where ω is angular frequency, k is the wave number, c is the speed of light in vacuum and n is the refractive index of the medium. From the above equation 3.1, it can be concluded that V_P is dependent on the refractive index of the material. As a pulse of light is generated by the interference of large number of sinusoidal waves and each of them has their own phase velocity. In a dispersive material, n varies with the wavelength and hence each component of wave packet will travel at different phase velocity. Therefore we need to define another velocity known as group velocity (V_G) to analyse the movement of the wave packets.

$$V_G = \frac{d\omega}{dk} = \frac{c}{n_G} \qquad (3.2)$$

And

$$n_G = n(\omega) + \omega\frac{dn(\omega)}{d\omega} \qquad (3.3)$$

Therefore the relation between the group velocity and the refractive index is give as

$$V_G = \frac{c}{n(\omega) + \omega\frac{dn(\omega)}{d\omega}} \qquad (3.4)$$

Thus by increasing the denominator of equation 3.4, we can reduce the group velocity of the wave packet.
The velocity of light wave can be reduced by interacting it with the propagating medium. The research on slow light is increasing day by day due to its huge application such as data synchronization, enhancement of light-matter interaction and optical forces, optical buffering, optical memories, optical signal processing, microwave photonics, and interferometric instruments [49-51]. With the help of slow light we can compress the optical signal and the optical energy in space which will reduce the device footprints and enhance the light-matter interaction. With the help of enhanced optical gain, absorption and nonlinearities per unit length, the size of various optical devices like lasers, detectors, amplifiers etc. can be reduced [41].
In this chapter, we are going to elaborate fundamentals of velocities of the light signal in section 3.2. After that in section 3.3, we are going to have an overview of various methods for the generation of slow-light used so far. Next in section 3.4, we will know the theory of stimulated Brillouin scattering (SBS) that we have used for our project to achieve slow light.

3.2. Velocities of light

Before having any discussion of altering the speed of light to achieve slow-light, we must be aware of various definitions of light velocities and their characteristics. Although there are atleast eight definitions of velocities light [52-54], here we are discussing only three: the photon velocity, the phase velocity, the group velocity.

3.2.1. Photon Velocity

When an electro-magnetic radiation is quantized in elementary particles to form packets of energy, such packets are known as photons. The velocity of such photons remains constant whether they are in any medium or inside a vacuum. This velocity is always constant and is determined by the speed of light in a vacuum $c \approx 3 \times 10^8$ m/s [55]**.** In case of propagation through a material the photons are absorbed and then re-emitted by its atoms**.** If this process is linear then the frequency of the photons remains constant but there will be a phase shift between the absorbed and re-emitted photon. However, during the propagation through free space inside the atoms, they move with the speed of light in a vacuum.

3.2.2. Phase Velocity

The phase velocity of any wave is defined as the velocity at which each point of a constant phase of wave (e.g. the maxima of a wave) travels. Assuming a complex electric field of a monochromatic wave with constant angular frequency $\omega = 2\pi f$ as a function of distance z and time t, given as in equation 3.5:

$$E(z,t) = \frac{1}{2}\left(E_0 e^{j(k(\omega)z-\omega t)} + c.c\right) \qquad (3.5)$$

where, E_0 is the amplitude of the propagating wave, $k(\omega) = k_0 \times n(\omega) = \omega/c \times n(\omega)$ is the frequency dependent wave number of the wave, and *c.c.* denotes the complex-conjugate part of the wave equation. The phase of this wave is denoted by φ and can be given as in equation 3.6:

$$\varphi(z,t) = k(\omega)z - \omega t \qquad (3.6)$$

As the phase remains constant while the wave propagates for certain small time interval *dt*, the differential of the above equation must be zero, *i.e.*

$$\frac{d\varphi}{dt} = k(\omega)\frac{dz}{dt} - \omega = 0 \qquad (3.7)$$

So from equation 3.7, the phase velocity (v_{ph}) of the propagating wave is given by:

$$v_{ph} = \frac{dz}{dt} = \frac{\omega}{k(\omega)} = \frac{c}{n(\omega)} \qquad (3.8)$$

From the above equation, it can be easily concluded that the phase velocity of any wave travelling in any medium is dependent on the refractive index of the medium and that refractive index is dependent on the frequency. If a wave consists of different frequencies, then each frequency component will have its own phase velocity through the dispersive media due to which the propagating wave will not retain its shape and it will large impact on the propagation of the pulse as a whole.

3.2.3. Group Velocity

The velocity of a wave is the velocity at which the overall shape of the waves' amplitudes known as modulation or envelope of the wave propagates through any medium. As we all know that an optical pulse comprises of large number of waves having different frequencies. So it is basically the modulation of carrier frequency. Let us consider two wave having same polarization and amplitude as equation 3.5 but having slightly different frequencies and wave numbers. The phases of the two waves are:

$$\varphi_1 = (k + \Delta k)z - (\omega + \Delta\omega)t \qquad (3.9)$$

$$\varphi_1 = (k - \Delta k)z - (\omega - \Delta\omega)t \qquad (3.10)$$

The sum of two waves is found to be:

$$E_s(z,t) = E_1(z,t) + E_2(z,t) = 2E_0 \cos(kz - \omega t)\cos(\Delta kz - \Delta\omega t) \qquad (3.11)$$

The first cosine factor in the above equation is the carrier of the pulse with phase velocity $v_{ph} = \omega/k$ and the second cosine factor is for the wave modulation of the pulse [56] which moves with group velocity. Similar to the derivation of the phase velocity, the group velocity v_g is given by:

$$v_g = \frac{dz}{dt} = \frac{d\omega}{dk} \tag{3.12}$$

In general it is known that the group velocity is dependent on group index (n_g). Thus the formula for group velocity of a wave having central frequency ω_0 is given as:

$$V_G = \frac{c}{n(\omega) + \omega \frac{dn(\omega)}{d\omega}} = \frac{c}{n_g} \tag{3.13}$$

In a vacuum, the group velocity is always equals to the phase velocity of the propagating wave because $n = 1$ for all the frequencies. Whereas in case of any medium, both are different because from the above equation we can see that v_g is not dependent only on frequency-dependent refractive index but also on the frequency-dependent slope of the refractive index i.e. $dn(\omega)/d\omega$. Hence if the medium is weak or non-dispersive, then only v_g will be equal to v_{ph}. An optical fiber, which is dispersive in nature, v_g will be dependent on refractive index slope. This refractive index slope varies with the frequency of the wave leads the frequency components of the wave to propagate with different velocities. It will lead to broadening of the pulse duration. The frequency-dependent alteration of group velocity is termed as *group velocity dispersion* (GVD) given by equation 3.14. [55]:

$$GVD = \frac{d}{d\omega}\left(v_g^{-1}\right) = \frac{1}{c}\left(2\frac{dn(\omega)}{d\omega} + \omega_0 \frac{d^2n(\omega)}{d\omega^2}\right) \tag{3.14}$$

Group velocity v_g is dependent on $\omega_0(dn(\omega)/d\omega)$, thus in case of normal dispersion medium where $(dn(\omega)/d\omega) > 0$, the group velocity decreases. The pulse gets decelerated and v_g becomes lesser than $v_{ph,}$ this phenomenon is known as *slow-light*.

3.3. Methods to achieve slow-light

Most of the methods to reduce the speed of a propagating wave are dependent on three factors, these factors are:

- methods that rely on the physical length of the waveguide or resonator,
- methods that alter the group velocity of the propagating signal wave and
- methods based on time-frequency-coherence of signals.

The slow light methods are classified as follows:

a) Alteration of Waveguide length

In this type of methods, the arrival time of the pulses is changed by changing the physical length of the propagation path. To achieve time delay in such methods, either the length of the single waveguide is increased or the cycle of the pulse inside a closed waveguide-loop is increased [57, 58] or resonators are used [59-62]. The only disadvantage of this method is that the time delay can't be varied continuously.

b) Alteration of group velocity

There are various methods which induce time delay in the propagating pulse by changing the group velocity of the pulse. It is basically used when the propagating material is highly dispersive. Some of the methods that use this phenomenon are: ring-resonators [59-62], semiconductor nanostructures [63], quantum well [64], semiconductor optical amplifiers (SOA) [65, 66], electromagnetically induced transparency (EIT) [67, 68], coherent population oscillation (CPO) [69, 70], stimulated Raman scattering (SRS) [71], stimulated Brillouin scattering (SBS) [72-74] and some other methods.

c) Time-frequency coherence

This class basically involves a novel technique known as quasi-light storage (QLS) [75]. In such methods, the coherence between the time and frequency representation of a propagating pulse is exploited. The main advantage of QLS method is that the light pulses can be stored for a short duration of time without any distortion.

Now we will briefly discuss some of the important methods that are used to introduce time delay in a propagating pulse and there advantages and disadvantages and then we will go through the method and the theory of stimulated Brillouin scattering (SBS) method, the method that we have used in our project.

3.3.1. Waveguide loops method

It is one of the simplest ways to introduce an optical pulse delay is to allow the pulse to pass through a delay line with a length of L, *e.g.* an optical waveguide or fiber [57]. When the pulse or the wave propagates through the waveguide, the group velocity of the wave will be dependent on the group index of the propagating medium. A time delay of $t_g = L/v_g$ is introduced in the pulse due to the fiber length L. In case we need to introduce a higher time delay, then we can pass the pulse through the same waveguide for more number of times. Suppose we pass the pulse for i number of times, then the total time delay introduced will be will be $i \times t_g$. The signal will propagate in the loop as long until it is switched to another path. Thus the signal can be stowed for small time duration if the attenuation of the waveguide is neglected.

Some other developments have been shown in this field, like if waveguides with different lengths can be coupled together by using switches [58]. Using different combination of waveguides or fiber loops, will introduce different time delay.
However this method was quite helpful to introduce time delay in the pulse, but it has some disadvantages like, the introduced time delay in this loop method is directly dependent on the physical length of the fiber. If the signal is placed in any loop then it can only be read out if the whole loop is completed. Hence in such cases time delay cannot be varied. Another problem associated with this loop method is attenuation of waveguides which reduces the signal power. It also introduces a high signal distortion due to waveguide dispersion. A lot of space is required to keep large network of waveguide loops.

3.3.2. Electromagnetically Induced Transparency (EIT)

As it is well known that the group velocity of a wave can be changed near a material resonance. Thus the very first experimentation on slow-light was done at strong absorption resonance that can be easily found in dilute gases. These gases have typically very small refractive indices on the order of $(n - 1) \approx 10^{-3}$ and at spectral boundaries of absorption, it varies and shows a normal dispersion. Hence the group index of such gases is also very large; of the order of 10^6 hence it leads $v_g \approx 300$ m/s [76]. In this method, due to absorption resonance, the attenuation is very high hence the light can be stored only for a short duration.
The above problem of storing the light for short duration can be easily removed by using coherent quantum interference effect of EIT. In this method, a narrow transparency window within absorption profile is created which allows the pulse to pass through it without experiencing any absorption and is associated with the change in group velocity of the propagating pulse. According to Kramers-Kronig relations, the transparency window causes the rapid variation of the refractive index and hence to the normal dispersion. Thus the value of v_g changes and the time delay depends on the efficiency of the transparency and on the slope of dispersion.
The EIT method was discovered by *Harris et al*. in a gas of atoms having three energy levels [77, 78]. It was basically based on the destructive quantum interference between the two probe field probes. The weaker probe field was tuned near one of the transition wavelengths (λ = 283 nm) of the absorption resonance and the second much stronger coupling field was tuned to some other transition wavelength (λ = 405.9 nm) so that it can induce a coherence between the ground state and the excited level and thus destructive quantum interference occurs between the two fields.
In the year 1999, *Hau et al*. used the EIT method to slow down the velocity of light pulses to 17 m/s [67]. They used a robust coupling field to an ultra-cold atomic cloud in the form of a Bose-Einstein condensate to generate the narrow transparency window within absorption resonance. It was basically the beginning of research on the topic of slow-light. Later *Hau et al*. achieved to stop the light pulse for 1 ms [79].

Despite of having good features, EIT method has some disadvantages:

a) The wavelength of the propagating pulse is required to adjust exactly the same as the wavelength of the material resonance. But in some of the cases these wavelengths are outside to the reach of those which are used nowadays in optical communication.

b) Application of EIT based slow-light systems is quite difficult due to their handling as exotic materials need extreme temperatures to be avoided any disturbance of quantum interference by any other effect and to achieve a large group index

3.3.3. Coherent Population Oscillations (CPO)

The CPO is the improved version of EIT method, it works in solid at room temperatures. Same as EIT, a narrow spectral window in absorption profile is required to change the group index of the propagating medium. In EIT method, quantum mechanical interference effect was involved between the electronic state wave functions whereas in CPO, two external laser beams are used for interference purpose. This quantum effect occurs in materials having two energy levels and shows a saturable absorption. A weak and a pump wave with slightly different frequency are applied to the medium, if both the fields are nearly resonant and the pump is strong, then their interaction will lead the atomic population to oscillate between the ground and the excited state. This result that the light is scattered efficiently from the pump into the probe and the absorption is decreased [80, 81]

This method has great advantages such that it can be realized in a large variety of materials at room temperatures and at the wavelengths that are used in optical. This method was quite helpful in achieving slow-light, fast-light and even negative group velocities in materials such as ruby [70], alexandrite and in erbium-doped optical fibers at pulse wavelengths of 1550 nm [69]. It is also used to achieve slow-light in semiconductor structures.

The problem related to this method is its narrow bandwidth, which is set by the inverse of the population recovery time. In some of the crystal, it is bounded to few KHz only, due to which it allows pulses of more than 1 ms [76].

3.3.4. Quasi-Light Storage (QLS)

QLS method is one of the newest methods to introduce time delay by storing the light pulses or train of light pulse that exploits the coherence between the time and spectral representation of the light signal. It basically works same as the real optical memory in which the data is stored as long as we want and only be released by giving the read signal. Initial investigation shows that the time delay of approximately 38 ns with several 5 bit patterns with a bit duration of 500 ps was achieved [75].

In this method, the input pulse is multiplied with the frequency comb in the frequency domain which leads to a pulse train with equidistant copies of the input pulse in time domains using Fourier transform. One of these copies is then haul out by a switch, which represents the time-delayed replica of the input pulse.
The main advantages of the QLS method are that it only uses standard components of telecommunication and also the time delay can be tuned in fine as well as in coarse range. Higher time delays are also easily available with tolerable optical powers and negligible signal distortion. This method is independent of the bit rate, the modulation format and the wavelength of the signals.

3.4. SBS based Slow-light

The main motive of our research work and this thesis is to design a new kind of PCF structure and then to analyse it for slow-light purpose based on SBS. So to know the method of SBS, we must need to go through the basics of SBS.

3.4.1. Brillouin scattering

In nineteen-twenties, there was a French physicist named *Leon Brillouin* who studied the interaction between light waves and the acoustic waves and hence this study was named after him as Brillouin scattering [55]. SBS is a nonlinear phenomenon which results with the interaction of the incident wave with the propagating material such as optical fiber. Until nineteen-sixties, there was no practical interest in SBS in optical fibers because the generation of nonlinear effects need high intensities of light which were available after the development of high efficient laser sources and fiber technologies.
Initially before SBS was examined by *Brillouin*, it takes a huge amount of power to transmit optical signal over a long distance to compensate the fiber attenuation. But after Brillouin scattering it become simpler to transmit signal over long distance as it requires milliwatts range of pump power in optical fiber. Hence SBS was made to use in optical components and networks [82-84].
Many applications were found that were benefitted with the properties of SBS [85]. Apart from generating slow- and fast-light, it was also used in fiber lasers [86], fiber amplifiers [87], optical fiber sensors [88] and tunable optical filters [89]. This all made the practical use of SBS in high resolution spectroscopy [90], millimetre wave generation in radio over fiber systems [91], in diagnostic tools for structural health monitoring [92].

3.4.2. Generation and Mode of operation

As we had already discussed that SBS is totally based on the interaction of a sufficiently strong incident light wave known as pump wave with the propagating medium as shown in fig 3.1. Due to fluctuation in the density of the optical fiber and the thermoelastic motions of the molecules, there is scattering of parts of the incident pump-wave into the backward

direction. This backscattered wave is known as stokes-wave. The backscattered stokes-wave superimposes with the pump-wave and builds up an electrical interference field. Due to the

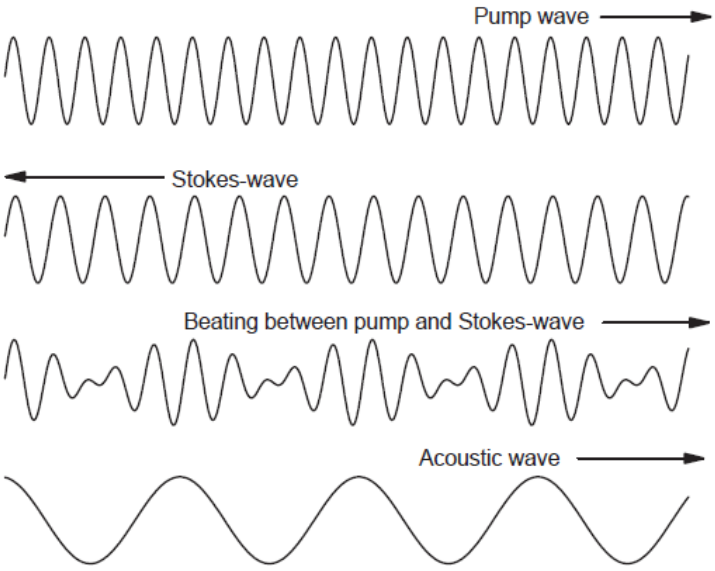

Fig.3.1: Interaction of waves in SBS (source: [55])

electrostriction, this interference pattern leads to periodic density modulation of the propagating medium which leads to the modulation of the refractive index and acts like a *Bragg* grating. If the Bragg condition is satisfied *i.e.* if the phases of the entire scattered or reflected wave are equal and interferes constructively, the optical retardation between the reflected wave components has to be a multiple of their wavelength [69] then more power of the pump wave will be backscattered. Due to this increase in power in backscattered wave, density modulation inside the medium increases and hence the stokes-wave increases exponentially and this process continues and more and more optical power of the pump-wave is backscattered and transferred to the stokes-wave. If the pump power exceeds a certain threshold power, the density modulation takes place by its own which means the Brillouin scattering became stimulated [55]. Till the pump power supply is sufficient and can compensate the decrease in pump power due to formation of acoustic wave, the SBS process will be self-preserving.

Density modulation of the propagating medium is also termed as acoustic wave because it propagates with the speed of sound in route to pump-wave. Due to this, there will be relative velocity in between the pump- and the acoustic wave which will shift the frequency or the wavelength of the stokes-wave by *Doppler effect* known as Brillouin shift [55].

Thus it can be concluded that SBS is basically a coupled interaction of three waves. Another condition for scattering process is that the conservation of momentum and energy law must be satisfied for their interaction. If f_p is the pump frequency, f_s is the frequency of stokes-wave and the acoustic wave frequency f_a, then they are related by [55]:

$$f_s = f_p - f_a \qquad (3.15)$$

It can be concluded from the above equation that frequency of the stokes-wave mediated by the acoustic wave is smaller than the frequency of the pump-wave. Hence f_a will be equal to f_B *i.e.* frequency of the Brillouin shift, given by equation 3.16.

$$f_a = f_B = \frac{2v_a n}{\lambda_p} \tag{3.16}$$

where v_a is the speed of sound in propagating medium, n is the refractive index of the medium, and λ_p is the pump wavelength. Apart from these variables, Brillouin shift also depends on the fiber type, the doping of the fiber core, the mechanical stress of the fiber and the ambient temperature [93].

3.4.3. Intensity equation and calculated parameters

Let, I_p be the pump intensity, I_s be the stoke wave intensity, g_B the Bruillion gain coefficient and α_P and α_S be the fiber losses at the pump and stokes frequencies then the coupled non-linear differential equation for pump and signal waves can be given as follows [30]

$$\frac{dI_p}{dz} = -g_B I_p I_s - \alpha I_p \tag{3.17}$$

$$-\frac{dI_s}{dz} = +g_B I_p I_s - \alpha I_s \tag{3.18}$$

If the fiber losses are zero *i.e.* $\alpha = 0$ then $\frac{d(I_P - I_S)}{dz} = 0$ and I_p - I_s remains constant along the fiber. Let the pump wave is undepleted so using the equation

$$I_p(Z) = I_p(0)e^{-\alpha Z} \tag{3.19}$$

We can solve the above equations and the solution is given as [94].

$$I_s(0) = I_s(L)\exp\left(\frac{g_B P_0 L_{eff}}{A_{eff}} - \alpha L\right) \tag{3.20}$$

where, A_{eff} is the effective mode area of the fiber, P_0 is the input pump power and can be given as $P_0 = I_p(0)\, A_{eff}$; α is the loss in the fiber, L is the real length of the fiber and L_{eff} is the effective length of the fiber which can be calculated using the formula

$$L_{eff} = \frac{[1 - \exp(-\alpha L)]}{\alpha} \tag{3.21}$$

and

$$g(\omega s) = \left(\frac{K_{g_0}|A_P|^2}{1 - j\frac{2(\omega_p - \omega_s - \Omega_B)}{\Gamma_B}}\right) \tag{3.22}$$

here, K is the polarization factor and depends on the polarization properties of the fiber. From previous results [24-26], we have used K = 0.667, which is appropriate for the fiber with low birefringence and very high polarization factor like tellurite, Γ_B is the SBS line width.
The real and imaginary part of $g(\omega_s)$ can be related using Kramers-Kronig Relation [95]

$$I_m[g(\omega_S)] = \frac{2}{\pi} \int_0^{\infty} \frac{\omega' R[g(\omega')]}{\omega'^2 - \omega_S^2} \, d\omega' \qquad (3.23)$$

At $\omega_p - \omega_s = \Omega_B$, the value of Bruillion gain coefficient will be maximum and can be written as [96]

$$g_B = \frac{2\pi n^7 {p_{12}}^2}{c{\lambda_P}^2 v_a \Delta v_B} \qquad (3.24)$$

where, n is the refractive index of the material of the fiber, p_{12} is the logitudnal elasto-optic coefficient, c is the velocity of the light, λ_p is the wavelength of the pump wave, v_a is the acoustic velocity, and v_B is the Brillouin Gain Bandwidth.
The minimum pump power required to initiate the SBS effect can be given as [97]

$$P_{min} = \frac{\alpha A_{eff} L}{K g_B L_{eff}} \qquad (3.25)$$

And the maximum pump power above which the output pulse is distorted is given by [97]

$$P_{max} = 21 \frac{A_{eff}}{K g_B L_{eff}} \qquad (3.26)$$

Where α is the loss coefficient of the fiber. The time delay which is induced due to SBS per unit length and per unit pump power by slow light fiber devices can be expressed as [98]

$$\frac{\Delta t_d}{L_{eff}} = \frac{P_P g_0 K}{\Gamma_B} \qquad (3.27)$$

Another important parameter to be calculate is Gain (G), and has been calculated using [99]

$$Gain[dB] = 10 \log\left(exp\left(g_B K \left(\frac{P_P}{A_{eff}}\right) L_{eff}\right)\right) \qquad (3.28)$$

hence, by varying the input Pump Power, both the time delay and Gain can be varied, thus we can see the variation of the time delay with respect to the Gain. The theoretical value of gain can be given by [98]

$$G_{th} = 4.34\left(\frac{g_B K \times 1mW \times L_{eff}}{A_{eff}}\right) \qquad (3.29)$$

Figure of merit (FOM) of the fiber can be given as [98]

$$FOM = \frac{Gain[dB]}{P_P L_{eff} n} = 4.34\left(\frac{g_B K L_{eff}}{A_{eff} n L}\right) \qquad (3.30)$$

3.5. Advantages and disadvantages of SBS based slow-light

Advantages

a) Power requirement in case of SBS is of milliwatts range for introducing a significant time-delay and since the time-delay is dependent directly on input pump power, the time-delay can be tuned over a wide range.
b) The phenomenon of SBS works at room temperature, for all wavelengths and especially at those which are used in optical communications. The designed fibers can be used as Brillouin and slow-light medium, hence it can be used for delaying the signals.
c) For slow-light purposes, the setups must be reliable and off-the-shelf telecommunication components are used which keeps the system clean, robust, cheap and easy to use.

Disadvantages

a) One of the disadvantages of the SBS based slow light is that the maximum achievable time-delay starts saturating at high pump powers. In the saturation region, the Brillouin gain and the time-delay does not increase.
b) There is a robust expansion of the pulse width with the delay in the pulse, causes the reduction in effective time delay. It is principally prompted by the narrow Brillouin bandwidth which acts like a bandpass filter and led to narrowing pulse spectrum.

3.6. Applications of slow-light

The main property of slow-light is to introduce a tuneable optical delay in any propagating pulse travelling through a conventional fiber of PCF. This property makes it suitable for various applications. Some of the applications are mentioned below:

3.6.1. Optical Buffers and Memories in Packed-Switched Networks

The realization of optical packet switches and routers is one of the major attractive applications of slow-light effect. Packet switching is basically a mode of communication in which the information is divided into blocks of various lengths, these blocks are termed as packets. Internet is an example of packet switched network in which packets are switched by different transmission paths by the router. The router is used to push the data from one input port to another output port. But the problem occurs when two packets arrive simultaneously to the router. It causes disputation and collision between the arrived packets. Thus storage of

one packet become necessary to process the other one [100]. The stored packet is released once the first packet has left the router. Figure 3.2 shows the whole process of data transmission by using a buffer.

The disadvantage of using conventional buffers is that it consists of fixed fiber length, which can provide fixed time delay. Due to this, there is immediate misalignment of the data systems and also constrains the adaption of different adaption rates. Hence these delay lines are not so useful for efficient and flexible all-optical buffering. A slow-light buffer fulfils the above requirement and offers an accurate time-delay required. It also offers highly précised allocation of each signal in a specific time slot with a dynamic adaptivity of the bit rate. Slow-light effect is also useful in optical synchronization and multiplexing of multiple data channels in different fiber.

Optical equalization is another major application of slow-light. As slow-light is based on gain or absorption resonances, the optical delay lines can be used additionally to equalize the power of different data channels. In the end another elementary operation of slow-light is the correlation in signal processing.

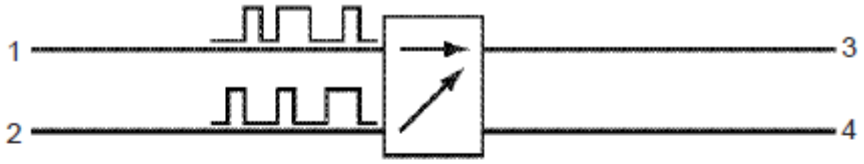

(a) Packet contention in a switch.

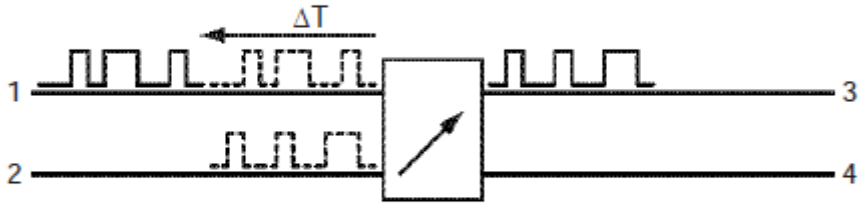

(b) Buffering of first packet and routing of second packet.

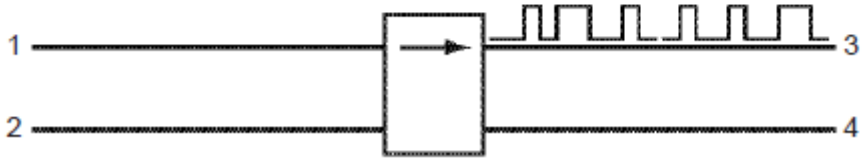

(c) Release and routing of first packet after second packed is routed.

Fig.3.2: Process of data transmission using a buffer (source: Ph.D. thesis: Ronny Henker, "Investigation of the Slow- and Fast-Light Effect on the Basis of Stimulated Brillouin Scattering for Application in Optical Communication and Information Systems" p: 27)

3.6.2. Spectroscopy and Interferometry

In case of time resolved spectroscopy, a pump probe configuration is used to characterize the material. In this, two short pulses having a time delay are sent to the sample, the first pulse changes the property of the sample and the other delayed pulse interrogates those changes. The delay provided to these pulses is basically achieved by mechanical components which

changes the length of the optical path. Due to this the precise adjustment of delay is very complicated and the system becomes bulky. A buffer equipped with slow-light effect can be used instead of mechanical component to have accurate and easy handling of the system [63]. The spectral resolution of the interferometer can be enhanced by increasing the length of the interferometer. But increasing the length means increase in size of the system. Thus another way to follow a long path is to slow down the signal over a fixed length. Therefore the resolution of the interferometer can be easily increased by a factor equal to the group index of the propagating medium and also the size of the spectroscopic interferometer can be easily reduced for a fixed resolution [101].

3.6.3. Phased-Array Antennas

Phased array devices also known as smart antennas are most important application of radio-frequency photonics. Is basically consists of a group of antennas, which vary the relative phases of the signals in such a way that the directional characteristics of the array shows a strong directivity in certain direction. By changing the phase relations of the phases of the signal, the direction of maximum gain is reconfigurable. There is a requirement of optical control to provide various radio services from one station smart antenna hence the electrical frequency dependent phase change between various signals can be replaced by wavelength independent time delay via slow-light element [63]

3.6.4. Quantum Information Processing

The quantum state in a quantum information processing is required to be stored for an adequate to permit it for quantum operations. This storage can be efficiently generated by using slow-light effect. Also by slowing down two pulses simultaneously in same material system quantum operation can be easily performed. The slower the light will be, the more it will get time to interact and thus close correlation state between the interacting photons and builds the basis of quantum processor [100].

Chapter 4
Stimulated Brillouin Scattering Based Slow Light Generation in Rectangular Core Photonic Crystal Fiber

4.1. Design of Proposed Photonic Crystal Fiber

The cross-sectional view of the proposed PCF design has been shown in Fig.4.1. It consists of an array of air holes arranged in rectangular lattice pattern in tellurite glass. The diameter of the innermost air holes is one and half the diameter of the rest of the air holes. The diameter of outer air holes is represented by '*d*' while the centre to centre distance of air holes (*i.e.* pitch) is taken as Λ.

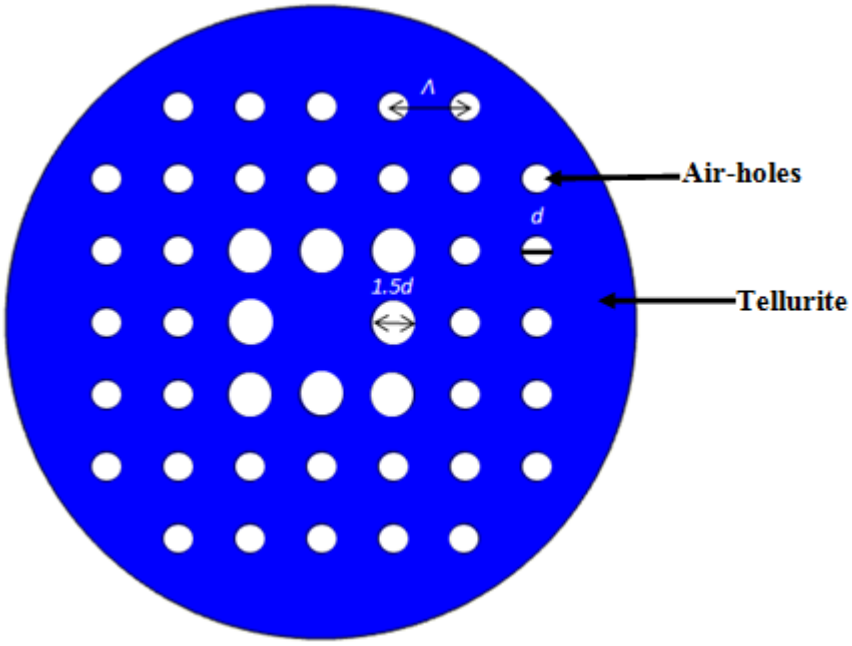

Fig.4.1: Cross-sectional view of proposed PCF having d = 1µm and Λ = 2.5µm.

4.2. Results and Discussion

The effective mode area is an important parameter for enhancing the nonlinear effects in the PCF structures. We have controlled the effective mode area (A_{eff}) of the PCF by tuning the filling fraction of the PCF structure. Filling fraction of a PCF is defined as the ratio of the diameter of the air holes to the pitch of the air holes (*i.e.* d/Λ). In our simulation, the diameter of the air holes in the cladding of the designed photonic crystal fiber has been reserved constant at 1 µm and the value of the d/Λ has been varied by changing the pitch of the air holes. The variation of the A_{eff} of propagating mode with the d/Λ has been illustrated in Fig.4.2. In this figure, it is observed that the A_{eff} decreases continuously on increasing the value of d/Λ. It is because of the enhancement of index contrast between core and cladding on decrease on the value of the Λ. The formula to find the Effective mode area of the fundamental mode of the designed PCF is given by:

$$A_{eff} = \frac{(\iint |E|^2 \, dx \, dy)^2}{(\iint |E|^4 dx \, dy)} \qquad (4.1)$$

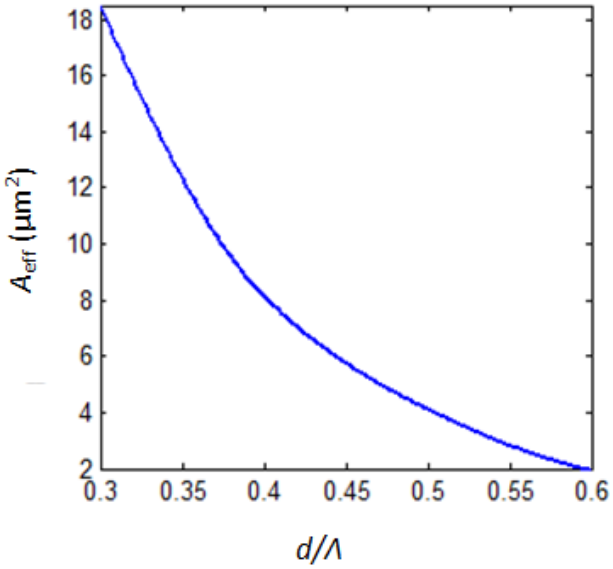

Fig.4.2: Variation of the effective mode area (A_{eff}) due to the air filling fraction of the PCF.

Another important feature of photonic crystal fiber is its confinement loss. From our simulation study, as shown in Fig.4.3, we have found that the value of the confinement loss of the propagating mode is 1.88 dB/m when d/Λ = 0.3 and it keeps on decreasing as the value of d/Λ increases. This decrease in confinement loss is due to the fact that as the value of pitch keeps on decreasing, the difference between core-cladding refractive index increases to higher confinement of the mode.

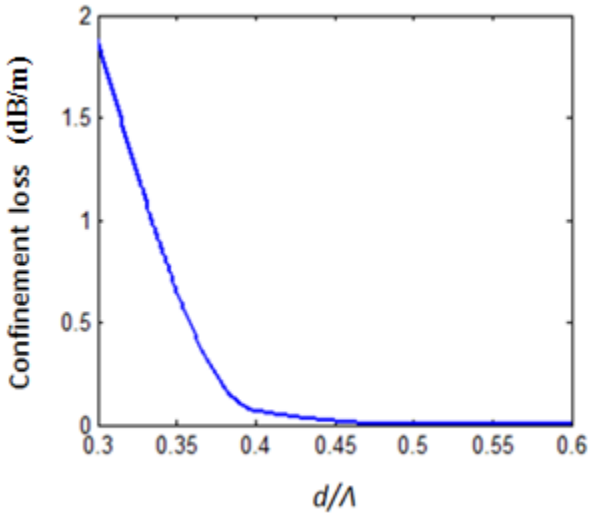

Fig.4.3: Variation of Confinement loss [dB/m] as a function of air filling fraction of the PCF.

Another parameter that we have calculated is non-linearity which is given by the Eq.

$$\gamma = \frac{2\pi n_2}{\lambda A_{eff}} \qquad (4.2)$$

where, n_2 (*i.e.* 2.5×10^{-19} m^2/W for tellurite glass [102]) is the non-linear refractive index of the material and λ is the wavelength of the input signal. In this study the wavelength is 1.55 nm. The variation of nonlinearity in proposed PCF structure has been shown in Fig.4.4. The nonlinearity increases on increasing the value of *d/Λ*. The structure offers the nonlinearity of 0.12 $m^{-1}W^{-1}$ for the PCF structure at *d/Λ* = 0.4.

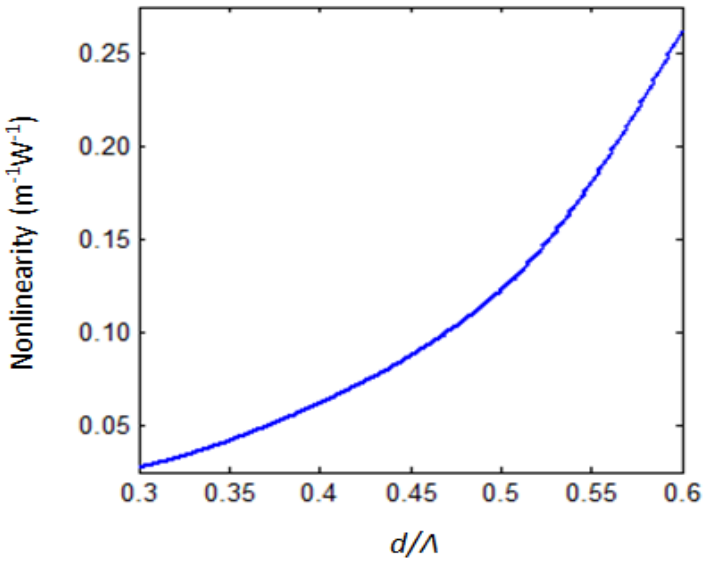

Fig.4.4: Variation of non-linearity with air filling factor of the PCF.

Table 4.1 shows the different values of effective mode area (A_{eff}), confinement loss and nonlinearity of the designed PCF for different values of air filling fraction i.e. *d/Λ*.

d/Λ	**A_{eff} (μm^2)**	**Confinement loss (dB/m)**	**Nonlinearity ($m^{-1}W^{-1}$)**
0.3	18.5	1.88	0.054
0.4	8.15	0.068	0.124
0.5	4.12	1.875×10^{-4}	0.245
0.6	1.93	5.03×10^{-7}	0.524

For the value of d/Λ = 0.4 we have found the A_{eff} to be 8.15 μm^2 and confinement loss to be 0.068 dB/m. Taking the fiber length of 100 m, the Bruillion gain coefficient, g_B = 1.6989×10^{-19} m/W, the fiber loss = 0.0558 dB/m (*i.e.* α = 0.01354/m), and the polarization factor, K = 0.667. We have calculated the P_{min} and P_{max} using the Equations (3.25, 3.26) which comes out to be P_{max} = 26.8 mW and P_{min} = 1.6 mW. Thus to get the time delay we had varied pump power P_p from 2 to 26 mW in our simulation.

The variation of time delay with the input pump power has been revealed in Fig.4.5. From this figure it can be concluded that the time-delay for input signal keeps on increasing as the input pump power increases. The value of time-delay for P_{min} (*i.e.* 2 mW) is found to be equal to 11.87 ns. The maximum value of the time-delay that can be obtained using the proposed PCF structure is 154.3 ns with pump power of 26 mW.

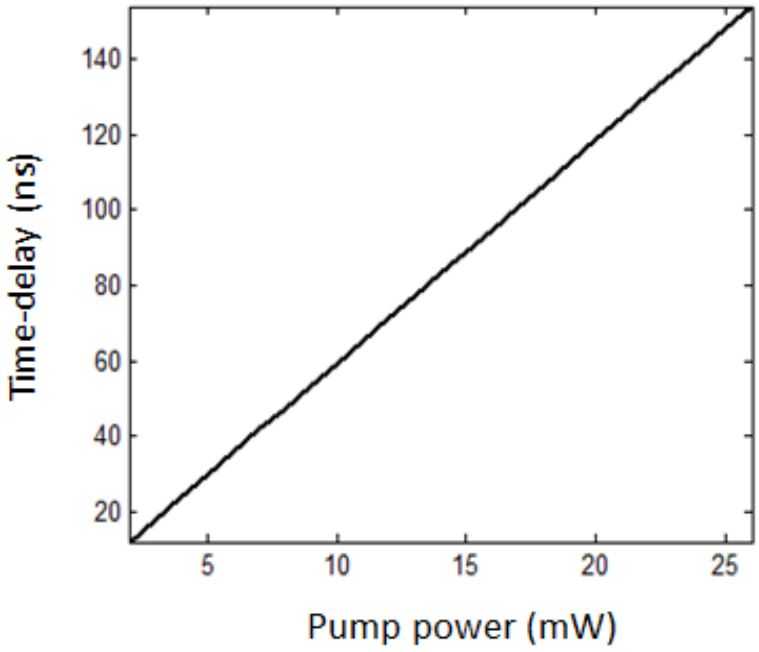

Fig.4.5: Maximum Time-delay as a function of input Pump power.

Figure 4.6 demonstrates the time-delay with the Brillouin gain (G). The time-delay keeps on increasing as the value of G increases. The minimum time-delay of 11.87 ns and maximum time-delay of 154.3 ns can be obtained with Brillouin gain of 17.62 dB and 19.07 dB respectively.

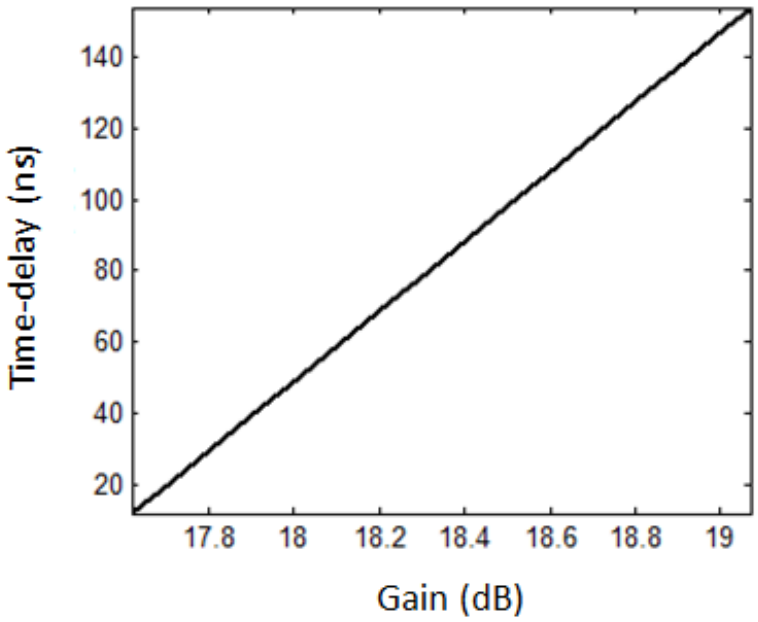

Fig.4.6: Maximum Time-delay as a function of Brillouin Gain (G)

This SBS induced time-delay also depends on the real length of the fiber. The maximum delay for 100 m long PCF for the input pump power of 26 mW is found to be around 154 ns. Finally, we have calculated the variation of SBS time delay with respect to the real length of the fiber as shown in Fig.4.7 for input pump power of 26 mW for fiber length varying from 0 to 500 m of length. Initially the time delay increases rapidly, but after certain value, it comes toward saturation. The maximum value of time delay for 500 m length of the fiber comes out to be around 210 ns. We also have calculated the values of theoretical gain and figure of merit (FOM) of proposed PCF structure which comes out to be 3.3958 dB and 0.0162 respectively.

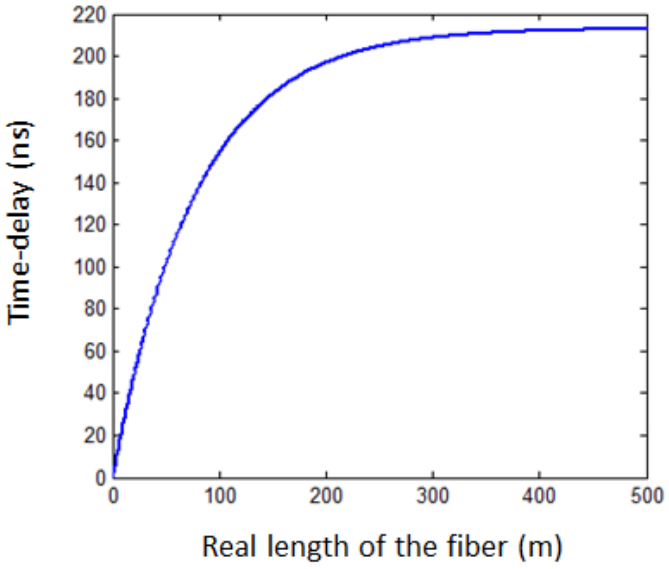

Fig.4.7: Time delay as a function of real length of the fiber.

Table 4.2 shows the various values of time-delay and the Brillouin gain for the given input pump power.

Input pump power (mW)	Time-delay (ns)	Brillouin Gain (dB)
2	11.87	17.62
5	29.67	17.81
10	59.33	18.11
15	89.00	18.41
20	118.70	18.71
25	148.30	19.01
26	154.30	19.07

4.3. Conclusion

A rectangular core tellurite photonic crystal fiber has been designed and analysed for tunable slow light generation based on stimulated Brillouin scattering. Various parameters like effective mode area, confinement loss, nonlinearity, and SBS time-delay have been calculated. The maximum time-delay of 154 ns has been found for the proposed photonic crystal fiber length of 100 m pumped with 26 mW pump power. Simulated results show that the time-delay in the photonic crystal fiber structure can be tuned with pump power as well as real fiber length and hence tunable slow-light features can be obtained from the structure. The proposed structure can be a good candidate for the various applications including the enhancement of the optical forces and light-matter interaction, optical buffering, optical memories, optical signal processing, and microwave photonics.

Chapter-5
SBS Based tunable slow-light in a novel graded-Index photonic crystal fiber: design and analysis

5.1. Design of proposed PCF

We have designed a graded index PCF for our study of SBS based slow-light. The cross-sectional view and the electric field pattern of the fundamental mode of the PCF have been shown in fig.5.1. We had used As_2Se_3 as the material of the PCF with air-holes arranged in rectangular manner. The diameters of the air-holes is kept increasing for graded index design. In our design, there are 3 layers of the air-hole with innermost layer of air holes having diameter of "*d*", second layer as "*1.5d*" and the outermost layer as "*2d*". The refractive index of the As_2Se_3 material has been used using the sellemier equation for a wavelength of 1.55 µm. The distance between the centres of the air holes is known as the pitch (Λ) of the PCF, which is kept constant in our design to 1 µm. The diameter of the air holes has been varied to find the effective mode area (A_{eff}) and the confinement loss.

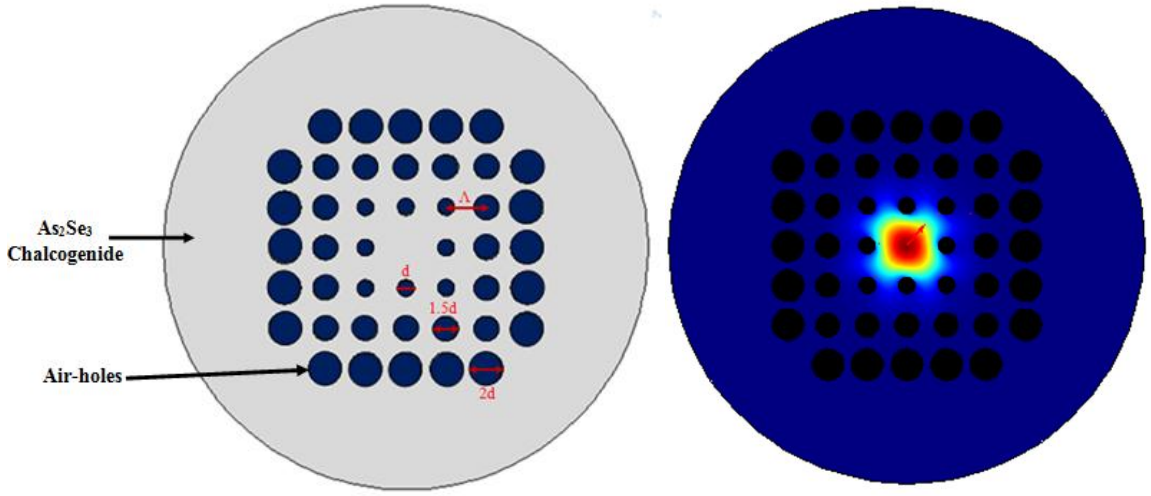

Fig.5.1: Design and electric field pattern of fundamental mode of the proposed graded-index PCF with Λ = 1 µm and d = 0.5 µm.

5.2. Analysis

The inherent properties of the As_2Se_3 chalcogenide material such as SBS linewidth (Γ_B) = 13.2 MHz, Brillouin gain coefficient (g_B) = 6.0×10^{-9} m/W has been taken from Reference [103]. The refractive index of the As_2Se_3 chalcogenide has been found by using Sellemier equation form Reference [104].

The first parameter calculated in our simulation is effective mode area (A_{eff}) of the designed graded index PCF. For the calculation of Aeff, we had varied the diameter (d) of the air holes. A_{eff} plays a very important role in the non-linear effects of the PCF. It depends on the Air filling fraction of the PCF. Air filling fraction of the PCF is defined as the ratio of the

diameter of the air-holes (*d*) and the distance between the centres of the air-hole i.e. pitch (Λ). Since, in our simulation the pitch is kept constant to 1 µm so the Air filling fraction (i.e. d/Λ) is mainly dependent on diameter (*d*) of the air holes. So as the diameter of the air-holes kept on increasing, the value of A_{eff} will decrease due to core size reduction. The variation of the A_{eff} has been shown in Fig.5.2. From our calculations, the value of A_{eff} is 1.72 μm^2 for d = 0.5 µm.

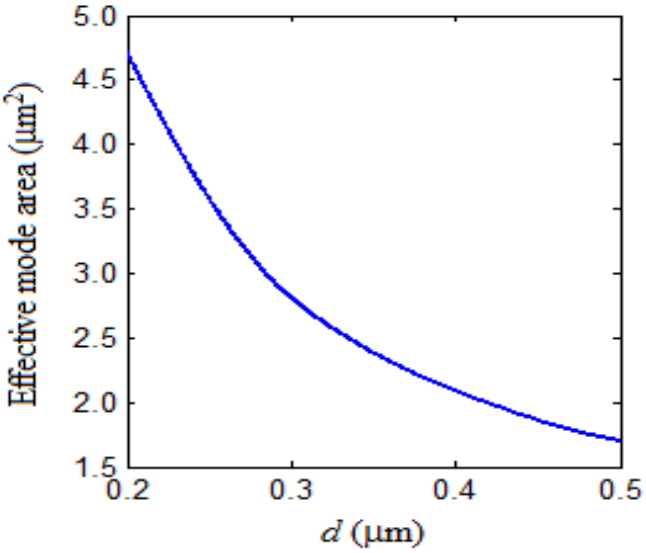

Fig.5.2: Variation of A_{eff} with diameter (*d*) of the air holes.

Another important parameter calculated by us is the Confinement loss of the designed graded index PCF. The confinement loss of the PCF basically depends on the confinement of light in core region and as the diameter of the air holes increases the difference between the refractive indices of the core and cladding also increases which leads to higher confinement of light and thus the confinement loss keeps on decreasing with increasing the diameter of the air-holes as shown in Fig.5.3.

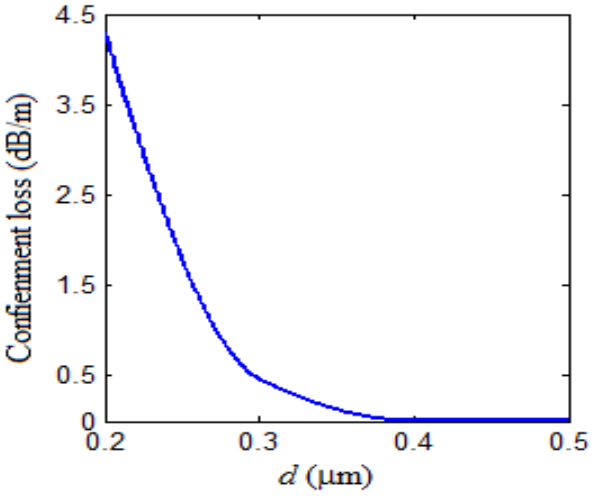

Fig.5.3: Variation of confinement loss with diameter (d).

d **(μm)**	A_{eff} **(μm^2)**	**Confinement loss (dB/m)**	P_{max} **(mW)**	P_{min} **(mW)**
0.2	4.72	4.30	27.24	0.25
0.3	2.81	0.46	16.21	0.14
0.4	2.09	3.83×10^{-5}	12.06	0.11
0.5	1.70	2.49×10^{-9}	9.81	0.09

Table 5.1: Values of A_{eff}, confinement loss and maximum and minimum power i.e. P_{max} and P_{min} for corresponding values of diameter (d) of the air-holes.

P_{max} and P_{min} are two important parameters for the calculation of time delay. They represent the maximum and the minimum allowable power that the PCF can tolerate. Figure 5.4 represents how the values of P_{max} and P_{min} vary with the increasing diameter of the air-holes. From which we can see that as the diameter of the air-holes increases, value of both P_{max} and P_{min} decreases, it is because of the confinement of the field within the smaller region, the power handling capacity of the PCF decreases. The value of P_{max} and P_{min} are 9.81 mW and 0.09 mW for d = 0.5 μm.

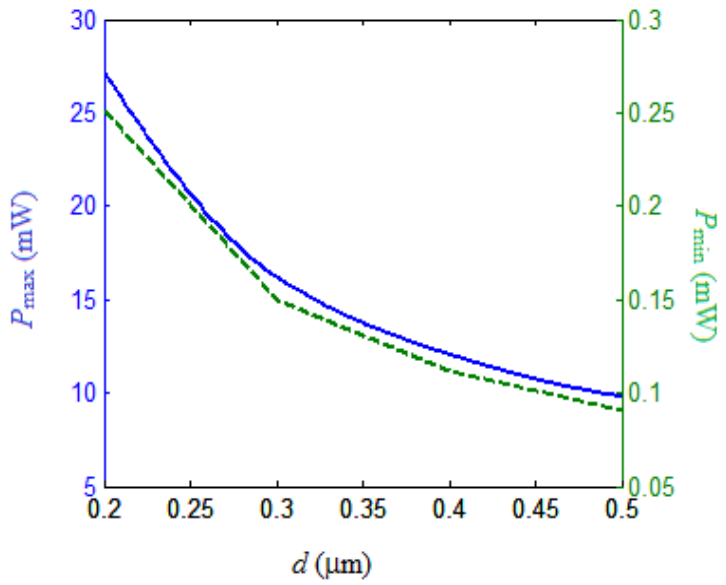

Fig.5.4: P_{max} and P_{min} varied with diameter (d).

From equation 3.27, the time-delay of the PCF is dependent on the input pump-power. The value of P_{max} and P_{min} are 9.81 mW and 0.09 mW for d = 0.5 μm. The variation of the time-delay with that of the input pump-power has been shown in Fig. 5.5 by varying the power from 0.8 mW to 9.8 mW. A maximum time-delay of 252.8 ns has been achieved for the

maximum input pump-power of 9.8 mW for 1 m long PCF. The time-delay increases with that of the input pump-power due to stimulated effect, where the optical fields substantially contribute to the phonon population.

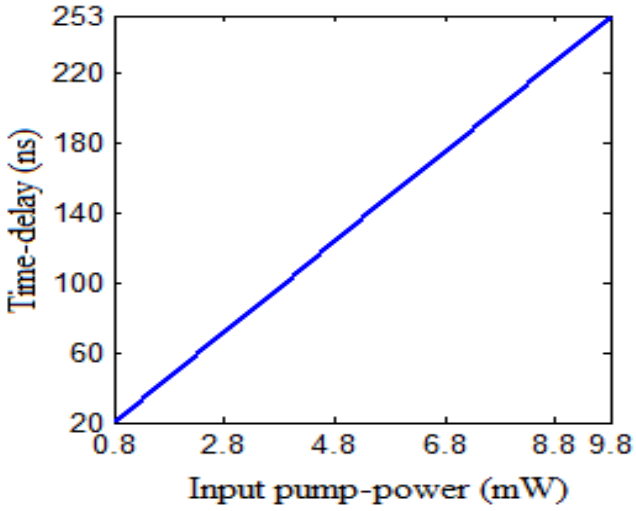

Fig.5.5: Variation of the Time-delay with input pump-power.

Figure 5.6 represents the variation of the maximum time-delay for different values of the diameter (d) of the air holes. From the figure we can easily conclude that the maximum time delay remains the same for all the values of the diameter, but the main advantage of increased diameter is that the input power required for the maximum time-delay has been reduced. As we can see P_{max} for d = 0.4 is 12.06 mW whereas the same P_{max} for d = 0.5 is 9.81 mW. For both the input pump-powers the maximum time-delay achieved is 252.8 ns. Hence it can be easily concluded that the PCF with more diameter of air holes is superior to PCF with lesser diameter of air holes because the fundamental mode is more confined and hence the losses are less, and the A_{eff} is also less.

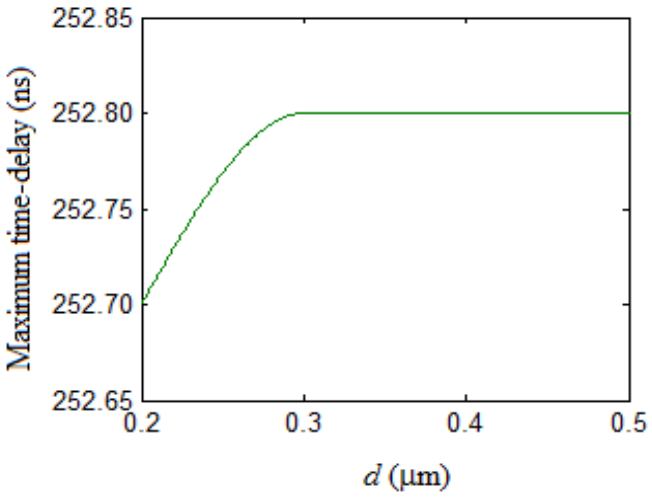

Fig.5.6: Maximum time-delay varying with respect to diameter of the air holes.

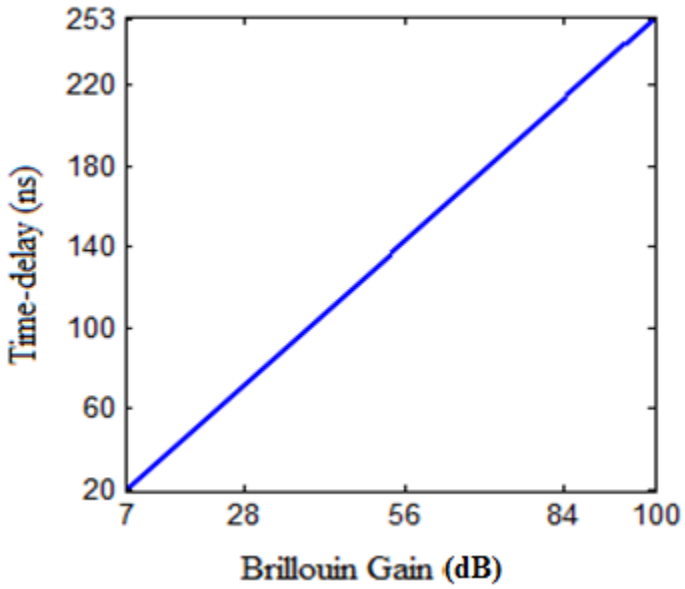

Fig.5.7: Time-delay varied with the Gain of the PCF

Brillouin Gain is also another important parameter for a PCF. As the diameter of the air-holes increases, the light beam is confined within the smaller core and hence there is a great enhancement in the Brillouin scattering which leads to greater Brillouin gain as shown in Fig.5.7. Table 5.2. represents the values of time-delay achieved and the Brillouin Gain for different values of the input pump-power.

Input pump-power (mW)	**Time-delay (ns)**	**Brillouin Gain (dB)**
0.8	20.64	7.76
2.8	72.23	28.21
4.8	123.80	48.66
6.8	175.40	69.11
8.8	227.00	89.56
9.8	252.80	99.78

The variation of the maximum time delay for d = 0.5 has been shown in Fig.5.8. From the figure we can conclude that initially the maximum time-delay keeps on increasing and then gets stable after some length. We have plotted the graph for the length of upto 10 m and a maximum time delay of around 1200 ns has been achieved.

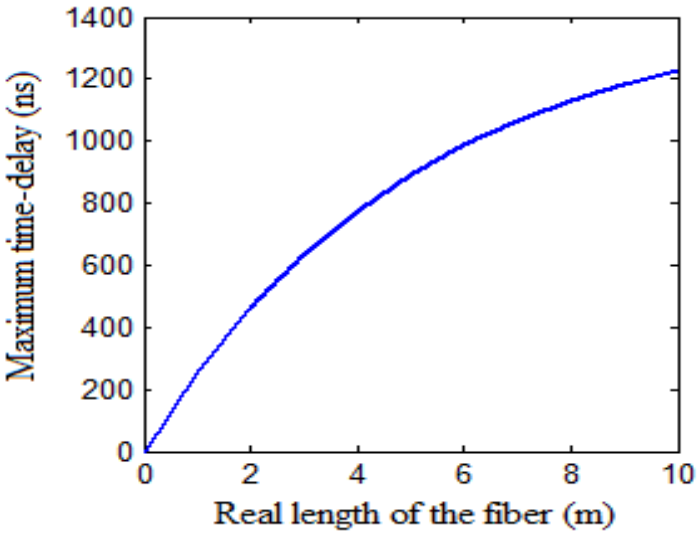

Fig.5.8: Maximum time-delay varied with real length of the fiber

5.3. Conclusion

A highly nonlinear As_2Se_3 chalcogenide photonic crystal fiber with rectangular core and the graded index has been designed and analysed by us for slow-light purpose based on SBS. Various parameters for slow light such as time-delay and Brillouin gain have been calculated. A maximum time-delay of 252.8 ns has been achieved for a small input power of 9.8 mW. Also a maximum Brillouin gain of 99.78 dB has been simulated with such a small power requirements. Our results has been found better than earlier reported works [105]; a higher time delay and very high Brillouin gain can be obtained with a small pump-power. Also the achieved time-delay can be tuned by varying the diameter or the pitch of the air-holes, hence the tunable features of the slow-light can be achieved. Hence the designed graded index PCF is expected to have the potential applications in realization of compact slow-light devices.

CHAPTER-6
Conclusion And Scope for future

In this project, we have designed two different photonic crystal fibers having different material and structure. The first PCF designed has a rectangular core with tellurite as a material. The time delay achieved for that design of 100 m long PCF was around 154 ns, and the input pump power required for this time-delay was 26 mW. The Brillouin Gain (G) for that PCF was 19 dB. Another PCF was designed for As_2Se_3 chalcogenide material and the air-holes were arranged in graded index manner. The length of the PCF was kept 1 m for all the calculation. In this PCF design, we have achieved a maximum time-delay of 252.8 ns for very low input pump power of 9.8 mW. The Brillouin Gain (G) was found to be around for 99.78 dB. It was found in our study that the time delay in the designed PCF can be tunned by tuning the diameter of the air holes or by changing the pitch of the designed PCF.

From our observation, it was found that a highly nonlinear material can induce more time delay as compared to that of the lower nonlinear material. Table 6.1: represents the various parameters and its comparison with both the designed PCFs.

Parameters Calculated	**Rectangular Core PCF with Tellurite Material**	**Graded Index PCF with As_2Se_3 Chalcogenide Material**
Effective Mode Area A_{eff} (μm^2)	4.12	1.70
Confinement Loss (dB/m)	1.875×10^{-4}	2.49×10^{-9}
Maximum Time Delay Achieved (ns)	154.30	252.8
Maximum Brillouin Gain (dB)	19.07	99.07

The investigation in this thesis shows that SBS is a promising tool for slow-light in optical fibers. It has the potential to realize all-optical short term fibers and buffers. As compared to other techniques, SBS has benefits of working at room temperature, small power consumption, wavelength independence, single-implementation and compatibility with existing optical fiber communication systems.

The future scope of this thesis is to improve the time-delay or the storage capacity of the PCF. There are several approaches like we can use highly nonlinear material to improve the time-delay performances, we can change the design of the PCF to reduce the effective mode area of the designed PCF.

The second approach is to reduce the pump-power required for a particular time-delay by using the above approaches. It will be helpful to reduce the length of the PCF. It can also be improve the storage capacity that can be used to investigate systems which are able to delay the pulses without distortions. It can be realized by a cascading of systems that can provide high time-delay but it leads to pulse broadening.

REFERENCES

1. K. C. Kao and G. A. Hockham, "Dielectric-fiber surface waveguides for optical frequencies," Proceedings of the IEEE 113, 1151-1158 (1966).
2. P. Vukusic and J. R. Sambles, "Photonic structures in biology," Nature 424, 852-855 (2003).
3. V. N. Melekhin and A. B. Manenkov, "Dielectric tube as a low-loss waveguide," Zhurnal Tekhnicheskoi Fiziki 38, 2113-2115 (1968).
4. E. Yablonovitch, "Inhibited Spontaneous Emission in Solid-State Physics and Electronics," Physical Review Letters 58, 2059-2059 (1987).
5. E. Yablonovitch, "Photonic band-gap structures," Journal of the Optical Society of America B 10, 283-295 (1993).
6. S. John, "Strong localization of photons in certain disordered dielectric superlattices," Physical Review Letters 58, 2486-2486 (1987).
7. J. C. Knight, T. Birks, P. S. J. Russell, and D. Atkin, "All-silica single-mode optical fiber with photonic crystal cladding," *Opt. Lett*. 21, 1547-1549 (1996).
8. J. C. Knight, T. Birks, P. S. J. Russell, and D. Atkin, "All-silica single-mode optical fiber with photonic crystal cladding: errata," *Opt. Lett.* 22, 484-485 (1997).
9. T. A. Birks, P. J. Roberts, P. St. J. Russell, D. M. Atkin, and T. J. Shepherd, "Full 2-D photonic bandgaps in silica/air structures," *Electron. Lett.* 31, 1941-1943 (1995).
10. J. C. Knight, J. Broeng, T. A. Birks, and P. S. J. Russell, "Photonic band gap guidance in optical fibers," Science 282, 1476-1478 (1998).
11. R. F. Cregan, B. J. Mangan, J. C. Knight, T. A. Birks, P. S. J. Russell, P. J. Roberts, and D. C. Allan, "Single-mode photonic band gap guidance of light in air," Science 285, 1537-1539 (1999).
12. J. C. Knight, T. A. Birks, R. F. Cregan, P. S. J. Russell, and J.-P. de Sandro, "Large mode area photonic crystal fibre," Electron. Lett. 34, 1347-1348 (1998).
13. J. K. Ranka, R. S. Windeler, and A. J. Stentz, "Efficient visible continuum generation in air-silica microstructure optical fibers with anomalous dispersion at 800 nm," Conference on Lasers and Electro-Optics CLEO '99, CPD8/1-CPD8/2 (1999).
14. A. Ortigosa-Blanch, J. C. Knight, W. J. Wadsworth, J. Arriaga, B. J. Mangan, T. A. Birks, and P. S. J. Russell, "Highly birefringent photonic crystal fibers", Opt. Lett. 25, 1325-1327 (2000).
15. J. E. Sharping, M. Fiorentino, A. Coker, P. Kumar and R. S. Windeler, "Four-wave mixing in microstructure fiber," Optics Letters 26, 1048-1050 (2001).
16. F. Benabid, J. Knight and P. Russell, "Particle levitation and guidance in hollow-core photonic crystal fiber," Optics Express 10, 1195-1203 (2002).
17. V. V. R. K. Kumar, A. George, J. Knight and P. Russell, "Tellurite photonic crystal fiber," Optics Express 11, 2641-2645 (2003).
18. A. Argyros, T. Birks, S. Leon-Saval, C. M. Cordeiro, F. Luan and P. S. J. Russell, "Photonic bandgap with an index step of one percent," Optics Express 13, 309-314 (2005).

19. P. Russell, "Photonic crystal fibers," Science 299, 358-362 (2003).
20. A. Bjarklev, J. Broeng, and A. S. Bjarklev, "Photonic Crystal Fibres," Kluwer Academic Publishers Boston (2003).
21. D. Kominsky, G. Pickrell, and R. Stolen, "Generation of random-hole optical fiber," Opt. Lett. 28, 1409-1411 (2003).
22. J. A. Harrington and C. C. Gregory, "Hollow sapphire fibers for the delivery of CO_2 laser energy," Optics Letters 15, 541-543 (1990).
23. T. Hidaka, "GeO_2-ZnO-K_2O glass as the cladding material of 940-cm^1 CO_2 laser-light transmitting hollow-core waveguide, "Journal of Applied Physics 53, 5484-5484 (1982).
24. T. Abel, J. Hirsch and J. A. Harrington, "Hollow glass waveguides for broadband infrared transmission," Optics Letters 19, 1034-1036 (1994).
25. T. G. Euser, G. Whyte, M. Scharrer, J. S. Y. Chen, A. Abdolvand, J. Nold, C. F. Kaminski and P. S. J. Russell, "Dynamic control of higher-order modes in hollow-core photonic crystal fibers," Optics Express 16, 17972-17981 (2008).
26. F. Benabid, J. C. Knight, G. Antonopoulos, and P. St. J. Russell, "Stimulated Raman scattering in hydrogen-filled hollow-core photonic crystal fiber," Science 298, 399-402 (2002).
27. F. Luan, A. K. George, T. D. Hedley, G. J. Pearce, D. M. Bird, J. C.Knight, P. St. J. Russell, "All solid photonic bandgap fiber," Opt. Lett. 29, 2369-2371 (2004).
28. S. J. A. Cerquiera, F. Luan, C. M. B. Cordeiro, A. K. George, J. C. Knight, "Hybrid photonic crystal fiber," Opt. Express 14, 926-931 (2006)
29. S. R. Petersen, T. T. Alkeskjold, J. Laegsgaard, "Degenerate four wave mixing in large mode area hybrid photonic crystal fibers," Opt. Exp. 21, 18111-18124 (2013).
30. G. P. Agrawal, "Nonlinear Fiber Optics," Third edition, Academic Press San Diego (2001).
31. G. P. Agrawal, "Fiber-Optic Communication Systems," Second Edition, John Wiley & Sons New York (1997).
32. D. Derickson, "Fiber Optic test and Measurement," Prentice Hall, New Jersey (1998).
33. J. C. Knight, J. Arriaga, T. A. Birks, A. Ortigosa-Blanch, W. J. Wadsworth, and P. St. J. Russell, "Anomalous dispersion in photonic crystal fiber," Photonics Technol. Lett. 12, 807-809 (2000).
34. T. A. Birks, J. C. Knight, and P. S. J. Russell, "Endlessly single-mode photonic crystal fiber," Opt. Lett., 22, 13, 961–963, (1997).
35. J. C. Knight, T. A. Birks, P. St. J. Russell, and J. P. de Sandro, "Properties of photonic crystal fiber and the effective index model," J. Opt. Soc. Am. A 15, 748-752 (1998).
36. J. C. Baggett, T. M. Monro, K. Furusawa and D. J. Richardson, "Comparative study of large mode holey and conventional fibers," Opt. Lett. 26, 1045-1047 (2001).
37. T. P. Hansen, J. Broeng, S. E. B. Libori, E. Knudsen, A. Bjarklev, J. R. Jensen, and H. Simonsen, "Highly birefringent index-guiding photonic crystal fibers", Photonics Technol. Lett. 13, 588-590 (2001).
38. A. Ortigosa-Blanch, A. Diez, M. Delgado-Pinar, J. L. Cruz, and M. V. Andres, "Ultrahigh birefringent nonlinear microstructured fiber", Photonics Technol. Lett. 16, 1667-1669 (2004).

39. M. Koshiba, and K. Saitoh, "Structural dependence of effective area and mode field diameter for holey fibers", Opt. Express 11, 1746-1756 (2003).
40. P. J. Roberts, F. Couny, H. Sabert, B. J. Mangan, D. P. Williams, L. Farr, M. W. Mason, A. Tomlinson, T. A. Birks, J. C. Knight, and P. S. J. Russell, "Ultimate low loss of hollow-core photonic crystal fibres", Opt. Express 13, 236-244 (2005).
41. T. Baba, "Slow light in photonic crystals" Nature Photon.2008, 2, 465-473.
42. D. J. Blumenthal, P. R. Pruncal, and J. R. Sauer, "Photonic packet switches: Architectures and experimental implementations," *Proc. IEEE* 82, 1650–1667 (1994).
43. G. M. Gehring, R. W. Boyd, A. L. Gaeta, D. J. Gauthier, and A. E. Willner, "Fiber-based slow-light technologies," *J. Lightwave Technol*. 26, 3752–3762, (2008)
44. J. T. Mok and B. J. Eggleton, "Expect more delays," *Nature*, 433, 811–812, (2005).
45. S. Rawal, R. K. Sinha, and R. M. De La Rue, "Slowlight miniature devices with ultra-flattened dispersion in silicon-on-insulator photonic crystal," *Opt. Exp.* 17, 13315–13325, (2009).
46. S. Rawal, R. K. Sinha, and R. M. De La Rue, "Silicon-on-insulator photonic crystal miniature devices with slow light enhanced third-order nonlinearities," *J. Nanophoton.* 6, 063504, (2012).
47. M. Santagiustina, G. Eisenstien, L. Thevenaz, J. Capmany, J. Mork, J. P. Reithmaier, A. De Rossi, S. Sales, K. Yvind, S. Cambrie and J. Bourderionnet, "Slow light devices and their applications to microwaves and photonics," *IEEE Photon. Soc. Newslett.*, 26, 5–12, (2012).
48. J. Capmany, I. Gasulla, and S. Sales, "Microwave photonics: Harnessing the speed of light," *Nature Photon.* 5, 731–733, (2011).
49. C. Monat, B. Corcoran, M. Ebnali-Heidari, C. Grillet, B. J. Eggleton, T. P. White, L. O'Faolain, and T. F. Krauss, "Slow light enhancement of nonlinear effects in silicon engineered photonic crystal waveguides," Opt. Express 17, 2944–2953 (2009).
50. S. Rawal, R.K. Sinha, R. De La Rue, "Silicon-on-insulator photonic crystal miniature devices with slow light enhanced third-order nonlinearities" J. Nanophoton. , 6, 0635-1-0635-12, (2012).
51. C. Monat, M. de Sterke, and B. J. Eggleton, "Slow light enhanced nonlinear optics in periodic structures", J. of Opt., vol. 12, p104003, (2010).
52. R. L. Smith, "The velocities of light," Am. J. Phys., vol. 38, no. 8, pp. 978-984, (1970).
53. S. C. Bloch, "Eighth velocity of light," Am. J. Phys., vol. 45, no. 6, pp. 538-549, (1977).
54. M. S. Bigelow, "Ultra-slow and superluminal light propagation in solids at room temperature," Ph.D. dissertation, University of Rochester, Rochester, USA, (2004).
55. T. Schneider, Nonlinear Optics in Telecommunications (Advanced Texts in Physics). Berlin, Heidelberg: Springer-Verlag, (2004).
56. P. W. Milonni, Fast Light, Slow Light and Left-Handed Light (Series in Optics and Optoelectronics). New York: Taylor & Francis Group, (2005).
57. R. Tucker, P.-C. Ku, and C. Chang-Hasnain, "Slow-light optical buffers: capabilities and fundamental limitations," J. Lightw. Technol., vol. 23, no. 12, pp. 4046-4066, (2005).
58. J. Spring and R. Tucker, "Photonic 2*2 packet switch with input buffers," Electr. Lett., vol. 29, no. 3, pp. 284-285, (1993).

59. J. B. Khurgin, “Optical buffers based on slow light in electromagnetically induced transparent media and coupled resonator structures: comparative analysis," J. Opt. Soc. Am. B, vol. 22, no. 5, pp. 1062-1074, (2005).
60. Q. Xu, P. Dong, and M. Lipson, “Breaking the delay-bandwidth limit in a photonic structure," Nature Physics, vol. 3, no. 6, pp. 406-410, (2007).
61. F. Xia, L. Sekaric, and Y. Vlasov, “Ultracompact optical buffers on a silicon chip," Nature Photonics, vol. 1, no. 1, pp. 65-71, (2007).
62. A. Melloni, F. Morichetti, C. Ferrari, and M. Martinelli, “Continuously tunable 1 byte delay in coupled-resonator optical waveguides," Opt. Lett., vol. 33, no. 20, pp. 2389-2391, (2008).
63. C. Chang-Hasnain, P.-C. Ku, J. Kim, and S.-L. Chuang, “Variable optical buffer using slow light in semiconductor nanostructures," Proceedings of the IEEE, vol. 91, no. 11, pp. 1884-1897, (2003).
64. P.-C. Ku, F. Sedgwick, C. J. Chang-Hasnain, P. Palinginis, T. Li, H. Wang, S.-W. Chang, and S.-L. Chuang, “Slow light in semiconductor quantum wells," Opt. Lett., vol. 29, no. 19, pp. 2291-2293, (2004).
65. A. Uskov, F. Sedgwick, and C. Chang-Hasnain, “Delay limit of slow light in semiconductor optical amplifiers," IEEE Photon. Technol. Lett., vol. 18, no. 6, pp. 731-733, (2006).
66. P. K. Kondratko, H. Su, and S.-L. Chuang, “Fast light using multiple cascaded quantum-well semiconductor optical amplifiers," in Conference on Lasers and Electro-Optics and Quantum Electronics and Laser Science (CLEO/QELS) 2007. Baltimore, MD, USA: OSA, May 2007, paper JWA41, (2007).
67. M. M. Kash, V. A. Sautenkov, A. S. Zibrov, L. Hollberg, G. R. Welch, M. D. Lukin, Y. Rostovtsev, E. S. Fry, and M. O. Scully, “Ultraslow group velocity and enhanced nonlinear optical effects in a coherently driven hot atomic gas," Phys. Rev. Lett., vol. 82, no. 26, pp. 5229-5232, (1999).
68. L. V. Hau, S. E. Harris, Z. Dutton, and C. H. Behroozi, Light speed reduction to 17 metres per second in an ultracold atomic gas," Nature, vol. 397, pp. 594-598, (1999).
69. A. Schweinsberg, N. N. Lepeshkin, M. S. Bigelow, R. W. Boyd, and S. Jarabo, “Observation of superluminal and slow light propagation in erbium-doped optical fiber," Europhys. Lett., vol. 73, no. 2, pp. 218-224, (2006).
70. M. S. Bigelow, N. N. Lepeshkin, and R. W. Boyd, “Observation of ultraslow light propagation in a ruby crystal at room temperature," Phys. Rev. Lett., vol. 90, no. 11, p. 113903, (2003).
71. J. Sharping, Y. Okawachi, and A. Gaeta, “Wide bandwidth slow light using a Raman fiber amplifier," Opt. Express, vol. 13, no. 16, pp. 6092-6098, (2005).
72. K. Y. Song, M. Gonzalez-Herraez, and L. Thevenaz, “Observation of pulse delaying and advancement in optical fibers using stimulated Brillouin scattering," Opt. Express, vol. 13, no. 1, pp. 82-88, (2005).
73. Y. Okawachi, M. S. Bigelow, J. E. Sharping, Z. M. Zhu, A. Schweinsberg, D. J. Gauthier, R. W. Boyd, and A. L. Gaeta, “Tunable all-optical delays via Brillouin slow light in an optical fiber," Phys. Rev. Lett., vol. 94, no. 15, p. 153902, (2005).

74. M. Gonzalez-Herraez, K. Y. Song, and L. Thevenaz, “Optically controlled slow and fast light in optical fibers using stimulated Brillouin scattering," Appl. Phys. Lett. vol. 87, no. 8, p. 081113, (2005).
75. S. Preuβler, K. Jamshidi, A. Wiatrek, R. Henker, C.-A. Bunge, and T. Schneider, “Quasi-light-storage based on time-frequency coherence," Opt. Express, vol. 17, no. 18, pp. 15 790-15 798, 2009, - announced as research highlight in Nature Photonics, vol. 3, no. 10, p. 555, Oct. (2009).
76. D. J. Gauthier, A. L. Gaeta, and R. W. Boyd, “Slow light: From basics to future prospects," Photonics Spectra, pp. 44-50, March (2006).
77. S. E. Harris, J. E. Field, and A. Imamoglu, “Nonlinear optical processes using electromagnetically induced transparency," Phys. Rev. Lett., vol. 64, no. 10, pp. 1107-1110, (1990).
78. S. E. Harris, J. E. Field, and A. Kasapi, “Dispersive properties of electromagnetically induced transparency," Phys. Rev. A, vol. 46, no. 1, pp. R29-R32, (1992).
79. C. Liu, Z. Dutton, C. H. Behroozi, and L. V. Hau, “Observation of coherent optical information storage in an atomic medium using halted light pulses," Nature, vol. 409, pp. 490-493, (2001).
80. J. B. Khurgin and R. S. Tucker, Eds., Slow Light: Science and Applications (Optical Science and Engineering), 1st ed. CRC Press, (2008).
81. P. W. Milonni, Fast Light, Slow Light and Left-Handed Light (Series in Optics and Optoelectronics). New York: Taylor & Francis Group, (2005).
82. H. Lee and G. Agrawal, “Suppression of stimulated Brillouin scattering in optical fibers using fiber Bragg gratings," Opt. Express, vol. 11, no. 25, pp. 3467-3472, (2003).
83. P. Weβels, P. Adel, M. Auerbach, D. Wandt, and C. Fallnich, “Novel suppression scheme for Brillouin scattering," Opt. Express, vol. 12, no. 19, pp. 4443-4448, (2004).
84. V. I. Kovalev and R. G. Harrison, “Suppression of stimulated Brillouin scattering in high-power single-frequency fiber amplifiers," Opt. Lett., vol. 31, no. 2, pp. 161-163, (2006).
85. S. P. Singh, R. Gangwar, and N. Singh, “Nonlinear scattering effects in optical fibers," Progress In Electromagnetics Research, vol. 74, pp. 379-405, (2007).
86. S. P. Smith, F. Zarinetchi, and S. Ezekiel, “Narrow-linewidth stimulated Brillouin fiber laser and applications," Opt. Lett., vol. 16, no. 6, pp. 393-395, (1991).
87. C. Atkins, D. Cotter, D. Smith, and R. Wyatt, “Application of Brillouin amplification in coherent optical transmission," Electr. Lett., vol. 22, no. 10, pp. 556-558, (1986).
88. X. Bao, D. J. Webb, and D. A. Jackson, “Combined distributed temperature and strain sensor based on Brillouin loss in an optical fiber," Opt. Lett., vol. 19, no. 2, pp. 141-143, (1994).
89. T. Tanemura, Y. Takushima, and K. Kikuchi, “Narrowband optical filter, with a variable transmission spectrum, using stimulated Brillouin scattering in optical fiber," Opt. Lett., vol. 27, no. 17, pp. 1552-1554, (2002).
90. J. Domingo, J. Pelayo, F. Villuendas, C. Heras, and E. Pellejer, “Very high resolution optical spectrometry by stimulated Brillouin scattering," IEEE Photon. Technol. Lett., vol. 17, no. 4, pp. 855-857, (2005).

91. T. Schneider, M. Junker, and D. Hannover, “Generation of millimetre-wave signals by stimulated Brillouin scattering for radio over fibre systems," Electr. Lett., vol. 40, no. 23, pp. 1500-1502, (2004).
92. L. Zou, X. Bao, F. Ravet, and L. Chen, “Distributed Brillouin fiber sensor for detecting pipeline buckling in an energy pipe under internal pressure," Appl. Opt., vol. 45, no. 14, pp. 3372-3377, (2006).
93. T. Schneider, D. Hannover, and M. Junker, “Investigation of Brillouin scattering in optical fibers for the generation of millimeter waves," J. Lightw. Technol., vol. 24, no. 1, pp. 295-304, (2006).
94. T.S. Saini, A. Kumar, R.K. Sinha, “Slow light generation in single-mode tellurite fibers” Journal of Modern Optics, 7. 508-513, (2015).
95. A. Zadok, A. Eyal, M. Tur, “Stimulated Brillouin scattering slow light in optical fibers” Appl. Opt., 50. E38-E49, (2011).
96. D. Cotter, “Observation of stimulated Brillouin scattering in lowloss silica fiber at 1.3 μm” Electron Lett., 18. 495-496, (1982).
97. R.G. Smith, “Optical Power Handling Capacity of Low Loss Optical Fibers as Determined by Stimulated Raman and Brillouin Scattering” Appl. Opt., 11. 2489-5865, (1972).
98. K.Y. Song, M.G. Herraez, L. Thevenaz, “Observation of pulse delaying and advancement in optical fibers using stimulated Brillouin scattering” Opt. Exp., 13. 82-88, (2005).
99. J.S. Sanghera, C.M. Florea, L.B. Shaw, P. Pureza, V.Q. Nguyen, M. Bashkansky, Z. Dutton, I.D. Aggarwal, ““Non-linear properties of chalcogenide glasses and fibers” J. Non-Crystaline Solids, 354. 462-467, (2008).
100. T. F. Krauss, “Why do we need slow light?" Nature Photonics, vol. 2, no. 8, pp. 448-450, (2008).
101. Z. Shi, R. W. Boyd, D. J. Gauthier, and C. C. Dudley, “Enhancing the spectral sensitivity of interferometers using slow-light media," Opt. Lett., vol. 32, no. 8, pp. 915-917, (2007).
102. V.V. Ravi, K. Kumar, A.K. George, J.C. Knight, P.St.J. Russell, “Tellurite photonic crystal fiber” Opt. Exp., 11, 2641-2645, (2003).
103. K. S. Abedin, “Observation of strong stimulated Brillouin scattering in single-mode As_2Se_3 chalcogenide fiber,” *Opt. Exp.* 13, 10266–10271, (2005).
104. W. Yuan, “2-10 μm mid-infrared super continuum generation in As2Se3photonics crystal fiber,” Laser Phys. Lett. 10, 095107, (2013).
105. T. S. Saini, A. Kumar, and R. K. Sinha, “Analysis and Design of Single-Mode As_2Se_3-Chalcogenide Photonic Crystal Fiber for Generation of Slow Light with Tunable Features,” *IEEE J. Sel. Topics Quant. Electron.* 22, 4900706, (2016).